Adaptive Control of Quadrotor Unmanned Aerial Vehicle with Time-Varying Uncertainties

IMIL HAMDA IMRAN[1,2], RUSTAM STOLKIN[3], ALLAHYAR MONTAZERI[1] .
[1]Department of Engineering, Lancaster University, Bailrigg, Lancaster, LA1 4YW, UK
[2]Applied Research Center for Metrology, Standards and Testing, King Fahd University of Petroleum and Minerals, Dhahran, 31261, Saudi Arabia
[3]Extreme Robotics Lab (ERL), School of Metallurgy and Materials, University of Birmingham, Edgbaston, Birmingham, B15 2TT, UK

Corresponding author: Allahyar Montazeri (e-mail: a.montazeri@lancaster.ac.uk).

ABSTRACT This paper studies the real-time parameter estimation and adaptive tracking control problem for a six degrees of freedom (6-DOF) quadrotor unmanned aerial vehicle (UAV) as an under-actuated system. A virtual proportional derivative (PD) is proposed to maintain the position dynamics. Two adaptive control schemes are designed and compared to maintain the attitude dynamics of the UAV while several parameters of the UAV are unknown. In the first scheme, a classical adaptive technique using the certainty equivalence principle is extended and designed for tracking control of the system with unknown time-varying parameters. To improve the performance of the first scheme, a new control technique is designed in the second scheme by proposing an additional continuous function to handle the unknown parameters. An additional robust term is designed in both schemes to handle the perturbation caused by unknown time-varying parameters. A rigorous analytical proof and numerical simulation analysis are provided to support the efficacy of the proposed controller.

INDEX TERMS Quadrotor, unmanned aerial vehicle, unknown time-varying parameter, classical adaptive scheme, certainty equivalence principle, adaptive control.

I. INTRODUCTION

RESEARCH on quadrotor UAV has attracted many attentions amongst both researchers and industries over the past decade. They are mostly useful for missions which are dull or hazardous for the human. For example, UAVs have found their way in nuclear decommissioning, volcano monitoring and data collection, geographical photography, precision agriculture, and creative industries [3, 24, 26]. Currently, autonomous operation and cognition of UAVs, either as an operation of a single UAV or as cooperation amongst several UAVs as a cyber-physical system is one of the hottest research areas from the control engineers' perspective [20, 29]. Many control strategies have been studied in different settings so far, and the main objective is to come with a design which is more realistic and suitable from the practical implementation point of view.

Quadrotor UAV is a nonlinear under-actuated system consisting of individual four rotors in a cross or plus configu-

ration. UAV has four control inputs to maintain six outputs with highly coupled states. There are three states related to translational motion that allow UAV to move in the lateral, vertical, backward and forward directions. The rest of the dynamic is related to the UAV attitude, i.e. roll, pitch and yaw angles. The main focus of the trajectory tracking problem in UAVs is to control the rotational dynamics. The primary reason is the under-actuated nature of UAV, for which the position tracking control problem is addressed by controlling UAV attitude dynamics.

One of the common issues in designing the controller for the rotational motions is the presence of nonlinearities in the system dynamics. Under this situation, a proper nonlinear controller plays an important role to handle the UAV movement in the full nonlinear operational range. Several investigations have been conducted to address the trajectory tracking problem, especially for rotational dynamics, in UAVs. Feedback linearization was proposed in [30, 32] is one

of the common techniques proposed for trajectory tracking problem in UAVs.

However, in many practical situations, several parameters of the UAV are unknown for the feedback control design. These uncertain parameters are likely to cause more technical challenges in designing the controller. There are two major research lines to handle this issue. The first approach is robust control technique. The idea behind this strategy is to design a feedback controller to dominate the unknown uncertainties in the system dynamics. As a result, the controller can handle the uncertainties within a certain bound. The disadvantage of this approach is that the uncertainty bound must be known in advance. One of the popular techniques using robust approach is the sliding mode control. This scheme is widely implemented in UAV applications as it is less sensitive to the disturbance, such as presented in [17, 31]. To compensate the effect of uncertain dynamics as well as unknown disturbances, while reducing the chattering problem in the sliding mode control, several efforts were presented in [4, 22, 23].

The second major research line is adaptive control, which is especially useful for systems with unknown parameters. Initially, the research in this direction is started with the classical adaptive approach using the certainty equivalence principle to handle the uncertain parameters. The idea behind this technique is to cancel the nonlinear terms containing the unknown constant parameter by estimating the unknown part. The adaptation law is derived using a Lyapunov like function such that the trajectory tracking objective is achieved. The perfect cancellation of the nonlinear term is achieved by driving the parameter estimation error to zero. This technique is simple in terms of implementation; however, it is limited for systems with unknown constant parameters. For some more information on this technique, refer to in [20].

Another adaptive scheme to handle uncertain parameters is the model reference adaptive control (MRAC). In this technique, an unknown constant parameter is estimated using a state predictor, as mentioned in [21]. Application of this technique for an unmanned vehicle can be found in [25]. However, MRAC has a major drawback that cannot guarantee the stability of the closed-loop system [1]. This issue was resolved by proposing the L_1 adaptive control scheme and designing a linear filter in the whole control structure [9]. This technique was studied further in [8] for collaborative UAVs. It should be noted that the estimated parameters in this technique do not converge necessarily to the actual parameters as the system was tuned for the worst-case condition. Since the mismatch between the estimated parameters and the actual values is used to update the parameters of the system, this approach is computationally expensive. Some results were investigated using state observer method for tracking control of UAV as presented in [27, 28]. Recently, an adaptive approach using the certainty equivalence principle was developed in [12, 13] for UAV with some unknown constant parameters.

Intelligent computation is another typical approach in the adaptive scheme to deal with unknown parameters. For ex-

ample, a genetic algorithm was proposed in [19] for robot manipulator, and a neural network (NN) was proposed in [6, 7] to handle the uncertainties for single and double integrator dynamics in the networked environment. There are two main issues in using intelligent computation. The first is that tracking control is not asymptotically achieved but with residual error. This is caused by the mismatch approximation of the nonlinear function. The second is that intelligent computation requires sophisticated hardware to estimate unknown parameters. As a result, from the perspective of UAV applications, this technique is limited to be implemented in the actual UAV systems.

To address the open issues in the classical adaptive control approach, immersion and invariance (I&I) was developed in [2, 18] to handle the unknown constant parameters. In this technique, the system was designed to satisfy the input to state stability (ISS) condition first without having unknown nonlinear terms in the system dynamics. The adaptive part was designed by adding a continuous function to the controller to guide the parameter estimation algorithm to the right direction. In this case, the stability was guaranteed by driving the mismatch estimation error to a specific manifold. It is worth noting that the stability condition here was derived by looking at the error dynamic for the parameter estimation rather than the closed-loop system dynamic. This was reasonably achieved by applying the ISS condition. This approach was designed to handle unknown constant parameters.

The I&I technique was proposed in [11, 16] to formulate the parameter estimation problem in UAVs. In this method, having the mismatch error between the estimated and the actual value of the parameters was necessary for the derivation of the adaptation law. Consequently, the method has a significant bottleneck to be applied in practical situations. To rectify this problem, in this paper, two techniques are proposed to control a quadrotor UAV with unknown time-varying parameters in the system dynamics. The control problem is more challenging due to the presence of the unknown time-varying gain in the control input structure. In the first scheme, an extended classical adaptive approach (ECAA) is developed to handle the time-varying parametric uncertainties in the system. The idea is to estimate the unknown parameters by proposing the certainty equivalence principle. This scheme suggests two steps to estimate the unknown parameters of the system dynamic. First, the controller is designed for the system under the ideal condition where all the system parameters are assumed to be known for the feedback control design. Then, in the second step, the unknown parameters of the system are replaced by their estimated values, generated as a result of the adaptation law. As mentioned above, this classical approach has an inherent drawback to estimate the unknown parameters of the system.

Inspired by the results reported in [2, 5, 14, 15], in the second scheme, a new adaptive technique is developed to handle multiple uncertain time-varying parameters of the UAV in the attitude dynamic part. The controller has a robust term to eliminate the effect of unknown parameters, where

the steady state parametric estimation error is not necessarily converging to zero. Compared to [2], here the ISS condition is relaxed, and the stability analysis is carried out on both the trajectory tracking and parameter estimation error dynamics. In this way, the necessity of having the mismatch error between the estimated parameter and the actual value is relaxed for both feedback control and parameter adaptation stages. This is a very important extension of the current techniques for the practical implementation of the algorithm. A virtual control using PD controller is utilized to track the position in the outer loop of the proposed nested control structure.

The remainder of this paper is organized as follows. The dynamics of UAV is presented in Section II. In Section III, the details relating to the two proposed adaptive schemes for the attitude dynamic control, including the position tracking control for the outer-loop are presented. The extensive numerical results are presented in Section IV to prove the efficacy of the proposed scheme. The paper is concluded in Section V with some suggestions for future research.

II. SYSTEM DYNAMICS OF UAV

Consider the general motion of the 6-DOF dynamic model of UAV expressed by the following states

$$\eta = \begin{bmatrix} \eta_1 \\ \eta_2 \end{bmatrix}, \quad \nu = \begin{bmatrix} \nu_1 \\ \nu_2 \end{bmatrix},$$

where $\eta_1 = \begin{bmatrix} x & y & z \end{bmatrix}^\top$ is a position vector consisting of forward (x), lateral (y) and vertical (z) states; $\eta_2 = \begin{bmatrix} \phi & \theta & \psi \end{bmatrix}^\top$ is an orientation vector consisting of roll (ϕ), pitch (θ) and yaw (ψ) states; $\nu_1 = \begin{bmatrix} u & v & w \end{bmatrix}^\top$ is a linear velocity; and $\nu_2 = \begin{bmatrix} p & q & r \end{bmatrix}^\top$ is an angular velocity vectors. The dynamic of the qaudrotor UAV is derived from the highly coupling between the inertial and body frames. This coupling can be expressed by the transformation matrices $J_1(\eta_2)$ and $J_2(\eta_2)$

$$J_1(\eta_2) = \begin{bmatrix} \cos\theta\cos\psi & \sin\phi\sin\theta\cos\psi - \cos\phi\sin\psi \\ \cos\theta\sin\psi & \sin\phi\sin\theta\sin\psi + \cos\phi\cos\psi \\ -\sin\theta & \sin\phi\cos\theta \end{bmatrix}$$
$$\begin{bmatrix} \cos\phi\sin\theta\cos\psi + \sin\phi\sin\psi \\ \cos\phi\sin\theta\sin\psi - \sin\phi\cos\psi \\ \cos\phi\cos\theta \end{bmatrix}$$

$$J_2(\eta_2) = \begin{bmatrix} 1 & \sin\phi\tan\theta & \cos\phi\tan\theta \\ 0 & \cos\phi & -\sin\phi \\ 0 & \frac{\cos\phi}{\cos\theta} & \frac{\cos\phi}{\cos\theta} \end{bmatrix}.$$

Assuming that $\cos\phi \neq 0$ and $\cos\theta \neq 0$, thus $J_1^\top(\eta_2) = J_1^{-1}(\eta_2)$. The dynamic coupling between position and orientation vectors can be represented by the following transformation

$$\dot{\eta}_1 = J_1(\eta_2)\nu_1, \quad \dot{\eta}_2 = J_2(\eta_2)\nu_2. \tag{1}$$

As derived in [16], the translational dynamic of the quadrotor UAV is expressed by

$$\ddot{\eta}_1 = -gz_e + J_1(\eta_2)\frac{u}{m}z_e - \frac{k_t}{m}\dot{\eta}_1, \tag{2}$$

and the attitude or rotational dynamics is

$$\dot{\nu}_2 = I_M^{-1}(-(\nu_2 \times I_M\nu_2) + \tau), \tag{3}$$

where g, u, m, and k_t are gravity acceleration, thrust force, mass, and translational drag coefficient, respectively. Vector $\tau = \begin{bmatrix} \tau_p & \tau_q & \tau_r \end{bmatrix}^\top$ is the torques acting in the body frame. Vector $z_e = \begin{bmatrix} 0 & 0 & 1 \end{bmatrix}^\top$ is the unitary vector in z direction and $I_M = \text{diag} \begin{bmatrix} I_x & I_y & I_z \end{bmatrix}$ is an inertia matrix. From (2) and (3), we can see that the number of degrees of freedom is higher than the number of control inputs, and hence the UAV is an under-actuated system.

The attitude dynamic in (3) with an additional external disturbance can be rewritten in the linearly parameterized form as

$$\dot{\nu}_2 = w_1 f(\nu_2) + w_2 \mathbf{1} + w_3 \tau, \tag{4}$$

where

$$w_1 = \text{diag} \begin{bmatrix} \frac{I_y - I_z}{I_x} & \frac{I_z - I_x}{I_y} & \frac{I_x - I_y}{I_z} \end{bmatrix}$$
$$w_3 = I_M^{-1}$$
$$f(\nu_2) = \begin{bmatrix} qr & pr & pq \end{bmatrix}^\top$$
$$\mathbf{1} = \begin{bmatrix} 1 & 1 & 1 \end{bmatrix}^\top.$$

Matrix w_2 is a time-varying additional disturbance acting on the body frame. The inertia parameters $I_x(t)$, $I_y(t)$ and $I_z(t)$ are unknown time-varying values satisfying the following assumptions.

Assumption 1: The inertia parameters $I_x(t)$, $I_y(t)$ and $I_z(t)$ are piecewise constant functions with time-varying switching time.

Both w_1 and w_3 are weighing matrices whose elements are constructed by the inertia parameters. As a result, w_1 and w_3 are also time-varying matrices. This is a practical assumption in many real life situations, for example when the inertia parameters are changing as a result of change in the UAV payload or when one or more components are damaged due to a fault. The effect of time-varying external disturbances on the attitude dynamic of the quadrotor is considered by the time-varying weight matrix w_2.

Assumption 2: The restriction on variations of the parameter $w_2(t)$ satisfies the following bounds for any $t \geq 0$

$$\underline{w}_2 \leq w_2(t) \leq \bar{w}_2$$
$$\delta = \frac{1}{2}|\bar{w}_2 - \underline{w}_2|,$$

where $\underline{w}_2$ and $\bar{w}_2$ are the minimum and maximum values of $w_2(t)$.

Remark 2.1: Here it is assumed that matrices $\underline{w}_2$ and $\bar{w}_2$ are unknown. The perturbation term $\sigma(t)$ is defined as $\sigma(t) = w_2(t) - l$, where l is a constant diagonal matrix. By choosing $l = \frac{1}{2}(\bar{w}_2 + \underline{w}_2)$, then under the Assumption 2, we have $|\sigma(t)| \leq \delta$ for any $t \geq 0$. Inspired by [5], it is worth noting that only the value of δ is assumed to be known for the feedback control design and the value of the parameter l is unknown as it appears only for the stability analysis of the feedback system and is not needed for the controller design.

III. PROPOSED CONTROL DESIGN

A UAV is an under-actuated system, in which four control inputs are used to control the six system states. All states are highly coupling between the translational and attitude dynamic of UAV. In this section, a nested control strategy for trajectory tracking of the quadrotor dynamic is designed. A PD controller is developed for the position tracking error in the outer loop. For inner loop, two adaptive control schemes are designed to control the attitude dynamic in the presence of uncertain parameters of the nonlinear system. The extended classical adaptive approach (ECAA) is proposed in the first step using the certainty equivalence principle. In this technique, the adaptive law is designed to handle parametric uncertainties. Nevertheless, in the second scheme, a new adaptive scheme is developed to improve the performance of the ECAA by adding a certain continuous differentiable function in the structure of the adaptive control design.

A. TRANSLATIONAL CONTROL DESIGN

In this section, the tracking controller for the translational dynamics is designed using a virtual PD controller. We define the tracking error of the system to be

$$\tilde{\eta}_1 = \eta_1 - \eta_{1_d}, \tag{5}$$

where $\tilde{\eta}_1$ and η_{1_d} are the error vector position and the desired vector position, respectively. The second order dynamics of (5) is expressed by

$$\ddot{\tilde{\eta}}_1 = -K_D \dot{\tilde{\eta}}_1 - K_P \tilde{\eta}_1. \tag{6}$$

The control gains K_P and K_D are selected to be positive definite matrices, then system dynamics (6) satisfies Routh-Hurwitz stability criterion by having $\lim_{t \to \infty} \tilde{\eta}_1(t) = 0$. We can rewrite the dynamics (5) as follows

$$\ddot{\eta}_1 = \ddot{\eta}_{1_d} - K_D(\dot{\eta}_1 - \dot{\eta}_{1_d}) - K_P(\eta_1 - \eta_{1_d}). \tag{7}$$

Inspired by [33], we define a virtual control input $U = \ddot{\eta}_1 = \begin{bmatrix} U_1 & U_2 & U_3 \end{bmatrix}^\top$ and substitute it in (2). As a result, we have

$$U = -gz_e + J_1(\eta_2)\frac{u}{m}z_e - \frac{k_t}{m}\dot{\eta}_1, \tag{8}$$

or

$$\frac{u}{m}z_e = J_1^{-1}(\eta_2)(U + gz_e + \frac{k_t}{m}\dot{\eta}_1). \tag{9}$$

From (9), we can verify that

$$(U_1 + \frac{k_t}{m}\dot{x})\cos\theta\cos\psi + (U_2 + \frac{k_t}{m}\dot{y})\cos\theta\sin\psi$$
$$-(U_3 + g + \frac{k_t}{m}\dot{z})\sin\theta = 0, \tag{10}$$

$$(U_1 + \frac{k_t}{m}\dot{x})(\sin\phi\sin\theta\cos\psi - \cos\phi\sin\psi)$$
$$+(U_2 + \frac{k_t}{m}\dot{y})(\sin\phi\sin\theta\sin\psi + \cos\phi\cos\psi)$$
$$+(U_3 + g + \frac{k_t}{m}\dot{z})\sin\phi\cos\theta = 0, \tag{11}$$

$$(U_1 + \frac{k_t}{m}\dot{x})(\cos\phi\sin\theta\cos\psi + \sin\phi\sin\psi)$$
$$+(U_2 + \frac{k_t}{m}\dot{y})(\cos\phi\sin\theta\sin\psi - \sin\phi\cos\psi)$$
$$+(U_3 + g + \frac{k_t}{m}\dot{z})\cos\phi\cos\theta = \frac{u}{m}. \tag{12}$$

The fact that $\cos\theta$ is non zero for any $t > 0$, then we can generate θ from (10) as follows

$$\theta = \arctan\left(\frac{(U_1 + \frac{k_t}{m}\dot{x})\cos\psi + (U_2 + \frac{k_t}{m}\dot{y})\sin\psi}{U_3 + g + \frac{k_t}{m}\dot{z}}\right). \tag{13}$$

By squaring both sides of (9), then we obtain

$$(\frac{u}{m}z_e)^\top(\frac{u}{m}z_e) = \left(J_1^{-1}(\eta_2)(U + gz_e + \frac{k_t}{m}\dot{\eta}_1)\right)^\top$$
$$\left(J_1^{-1}(\eta_2)(U + gz_e + \frac{k_t}{m}\dot{\eta}_1)\right)$$
$$= \left(U + gz_e + \frac{k_t}{m}\dot{\eta}_1\right)^\top\left(U + gz_e\right.$$
$$\left. + \frac{k_t}{m}\dot{\eta}_1\right). \tag{14}$$

As a result

$$\frac{u}{m} = \left((U_1 + \frac{k_t}{m}\dot{x})^2 + (U_2 + \frac{k_t}{m}\dot{y})^2\right.$$
$$\left. + (U_3 + g + \frac{k_t}{m}\dot{z})^2\right)^{1/2} \tag{15}$$

From (11) and (12), we have

$$\frac{u}{m}\sin\phi = (U_1 + \frac{k_t}{m}\dot{x})\sin\psi - (U_2 + \frac{k_t}{m}\dot{y})\cos\psi \tag{16}$$

By substituting (15) to (16), we can derive ϕ as follows

$$\phi = \arcsin\left(((U_1 + \frac{k_t}{m}\dot{x})\sin\psi - (U_2 + \frac{k_t}{m}\dot{y})\cos\psi)\right.$$
$$\left((U_1 + \frac{k_t}{m}\dot{x})^2 + (U_2 + \frac{k_t}{m}\dot{y})^2\right.$$
$$\left.\left. + (U_3 + g + \frac{k_t}{m}\dot{z})^2\right)^{-1/2}\right). \tag{17}$$

The total thrust can be generated from (12) as expressed by

$$u = m\left((U_1 + \frac{k_t}{m}\dot{x})(\cos\phi\sin\theta\cos\psi + \sin\phi\sin\psi)\right.$$
$$+ (U_2 + \frac{k_t}{m}\dot{y})(\cos\phi\sin\theta\sin\psi - \sin\phi\cos\psi)$$
$$\left. + (U_3 + g + \frac{k_t}{m}\dot{z})\cos\phi\cos\theta\right). \tag{18}$$

By following a similar way, we can calculate ϕ_d and θ_d from (17) and (13)

$$\phi_d = \arcsin\left(((U_1 + \frac{k_t}{m}\dot{x}_d)\sin\psi_d - (U_2 + \frac{k_t}{m}\dot{y}_d)\right.$$
$$cos\psi_d)\left((U_1 + \frac{k_t}{m}\dot{x}_d)^2 + (U_2 + \frac{k_t}{m}\dot{y}_d)^2\right.$$
$$\left.\left. + (U_3 + g + \frac{k_t}{m}\dot{z}_d)^2\right)^{-1/2}\right) \tag{19}$$

$$\theta_d = \arctan\left(\frac{(U_1 + \frac{k_t}{m}\dot{x}_d)\cos\psi_d + (U_2 + \frac{k_t}{m}\dot{y}_d)\sin\psi_d}{U_3 + g + \frac{k_t}{m}\dot{z}_d}\right). \tag{20}$$

B. ATTITUDE CONTROL DESIGN

The main contribution of the paper is presented in this section. The presence of uncertain parameters in the attitude dynamics may cause a challenging problem in designing the attitude controller. If all system parameters are known for the feedback control design, we can cancel the nonlinear terms by proposing a simple feedback linearization method. However, in many practical situations, several parameters of the UAV are often unknown. The problem becomes more complicated for unknown time-varying parameter cases. Consequently, a proper controller such as adaptive techniques is required to handle the uncertainties. In this paper, all parameters of the attitude dynamics are unknown and time-varying. ECAA and a new approach are designed and compared to handle this issue.

Before presenting the main results, we define the desired trajectory as $\nu_{2_d} = \begin{bmatrix} p_d & q_d & r_d \end{bmatrix}^\top$. The trajectory error can be calculated by $e = \nu_2 - \nu_{2_d}$. Therefore, the tracking dynamics error can be written as

$$\dot{e} = w_1 f(\nu_2) + w_2 \mathbf{1} + w_3 \tau - \dot{\nu}_{2_d}. \tag{21}$$

The tracking control is deemed to be successful if

$$\lim_{t\to\infty} e(t) = 0. \tag{22}$$

Now, we define an ideal reference model without uncertainties that leads to desired trajectory ν_{2_d} as represented by

$$\dot{\hat{\nu}}_2 = -K_1(\hat{\nu}_2 - \nu_{2_d}), \tag{23}$$

with a stable tracking error dynamics

$$\dot{e}_d = -K_1(\hat{\nu}_2 - \nu_{2_d}) - \dot{\nu}_{2_d}, \tag{24}$$

where K_1 is a positive-definite constant matrix, $\hat{\nu}_2 = \begin{bmatrix} \hat{p} & \hat{q} & \hat{r} \end{bmatrix}^\top$ is the state of reference model, and $e_d = \hat{\nu}_2 - \nu_{2_d}$. From (21) and (24), we can write the new tracking error dynamics as

$$\dot{\tilde{\nu}}_2 = K_1(\hat{\nu}_2 - \nu_{2_d}) + w_1 f(\nu_2) + w_2 \mathbf{1} + w_3 \tau, \tag{25}$$

where $\tilde{\nu}_2 = \nu_2 - \hat{\nu}_2$. Before presenting the main results, we define

$$\underline{\nu}_2 = \text{diag}(\nu_2),\ \tilde{\underline{\nu}}_2 = \text{diag}(\tilde{\nu}_2)$$
$$E = \text{diag}(e),\ F(\nu_2) = \text{diag}(f(\nu_2))$$
$$\chi(\tilde{\nu}_2) = \begin{bmatrix} \chi_1 & \chi_2 & \chi_3 \end{bmatrix}^\top,\ \chi(\tilde{\underline{\nu}}_2) = \text{diag}(\chi(\tilde{\nu}_2)),$$

where

$$\chi_1 = \text{sgn}(p - \hat{p})$$
$$\chi_2 = \text{sgn}(q - \hat{q})$$
$$\chi_3 = \text{sgn}(r - \hat{r}),$$

1) Extended classical adaptive approach

In the first scheme, we present a classical adaptive approach to handle the uncertain parameters in the attitude dynamics. The unknown matrices of w_1, w_2 and w_3 are estimated by $\hat{w}_1$, $\hat{w}_2$ and $\hat{w}_3$, respectively, where $\tilde{w}_1 = \hat{w}_1 - w_1$, $\tilde{w}_2 = \hat{w}_2 - l$, and $\tilde{w}_3 = \hat{w}_3 - w_3^{-1}$; and constant l is defined in Remark 2.1. The extended classical adaptive scheme is presented in Theorem 3.1.

Theorem 3.1: (**ECAA**) Consider the attitude dynamics (4), under the Assumptions 1 and 2, the proposed control law is designed as

$$\tau = -\hat{w}_3\big(K_1 e + K_2 \chi(\tilde{\nu}_2) + \hat{w}_1 f(\nu_2) + \hat{w}_2 \mathbf{1}\big), \tag{26}$$

where $\hat{w}_1$, $\hat{w}_2$ and $\hat{w}_3$ are updated by the following adaptation laws

$$\dot{\hat{w}}_1 = \Gamma_1 F(\nu_2)\tilde{\underline{\nu}}_2,$$
$$\dot{\hat{w}}_2 = \Gamma_2 \tilde{\underline{\nu}}_2,$$
$$\dot{\hat{w}}_3 = \Gamma_3 \tilde{\underline{\nu}}_2(K_1 E + K_2 \chi(\tilde{\nu}_2) + \hat{w}_1 F(\nu_2) + \hat{w}_2), \tag{27}$$

for some selection of $\alpha, \Gamma_1, \Gamma_2, \Gamma_3 > 0$, $K_1 > \frac{\alpha}{2}I_3$ and $K_2 \geq \frac{1}{2\alpha}\delta^2$. Then the time-derivative of

$$V_{\tilde{\nu}_2 \tilde{w}_1 \tilde{w}_2 \tilde{w}_3} = \frac{1}{2}\tilde{\nu}_2^\top \tilde{\nu}_2 + \text{tr}\Big(\frac{1}{2}\Gamma_1^{-1}\tilde{w}_1^2 + \frac{1}{2}\Gamma_2^{-1}\tilde{w}_2^2 + \frac{1}{2}\Gamma_3^{-1}w_3\tilde{w}_3^2\Big), \tag{28}$$

along the closed-loop system (4)+(26)+(27) is

$$\dot{V}_{\tilde{\nu}_2 \tilde{w}_1 \tilde{w}_2 \tilde{w}_3} \leq -\tilde{\nu}_2^\top(K_1 - \frac{\alpha}{2}I_3)\tilde{\nu}_2 - \tilde{\nu}_2^\top(K_2 - \frac{1}{2\alpha}\delta^2)\chi(\tilde{\nu}_2) \leq 0, \tag{29}$$

Proof: The dynamics error of closed-loop system (4)+(26)+(27) can be written as

$$\dot{\tilde{\nu}}_2 = K_1(\hat{\nu}_2 - \nu_{2_d}) + w_1 f(\nu_2) + w_2 \mathbf{1} - w_3 \hat{w}_3$$
$$(K_1 e + K_2 \chi(\tilde{\nu}_2) + \hat{w}_1 f(\nu_2) + \hat{w}_2 \mathbf{1})$$
$$= K_1(\hat{\nu}_2 - \nu_{2_d}) + w_1 f(\nu_2) + w_2 \mathbf{1} - w_3$$
$$(\tilde{w}_3 + w_3^{-1})\big(K_1 e + K_2 \chi(\tilde{\nu}_2) + \hat{w}_1 f(\nu_2) + \hat{w}_2 \mathbf{1}\big)$$
$$= K_1(\hat{\nu}_2 - \nu_{2_d}) + w_1 f(\nu_2) + w_2 \mathbf{1} - w_3 \tilde{w}_3$$
$$(K_1 e + K_2 \chi(\tilde{\nu}_2) + \hat{w}_1 f(\nu_2) + \hat{w}_2 \mathbf{1})$$
$$- K_1 e - K_2 \chi(\tilde{\nu}_2) - \hat{w}_1 f(\nu_2) - \hat{w}_2 \mathbf{1}$$
$$= -K_1 \tilde{\nu}_2 - K_2 \chi(\tilde{\nu}_2) - \tilde{w}_1 f(\nu_2) - (\tilde{w}_2 + \sigma)\mathbf{1}$$
$$- w_3 \tilde{w}_3(K_1 e + K_2 \chi(\tilde{\nu}_2) + \hat{w}_1 f(\nu_2) + \hat{w}_2 \mathbf{1}). \tag{30}$$

Direct calculation shows that the time-derivative of $V_{\tilde{\nu}_2 \tilde{w}_1 \tilde{w}_2 \tilde{w}_3}$ is

$$\dot{V}_{\tilde{\nu}_2 \tilde{w}_1 \tilde{w}_2 \tilde{w}_3} = \tilde{\nu}_2^\top \dot{\tilde{\nu}}_2 + \text{tr}\Big(\Gamma_1^{-1}\tilde{w}_1 \dot{\hat{w}}_1 + \Gamma_2^{-1}\tilde{w}_2 \dot{\hat{w}}_2 + \Gamma_3^{-1}w_3\tilde{w}_3 \dot{\hat{w}}_3\Big)$$
$$= \tilde{\nu}_2^\top\Big(-K_1\tilde{\nu}_2 - K_2\chi(\tilde{\nu}_2) - \tilde{w}_1 f(\nu_2)$$
$$- \tilde{w}_2 \mathbf{1} + \sigma \mathbf{1} - w_3 \tilde{w}_3\big(K_1 e + K_2 \chi(\tilde{\nu}_2)$$
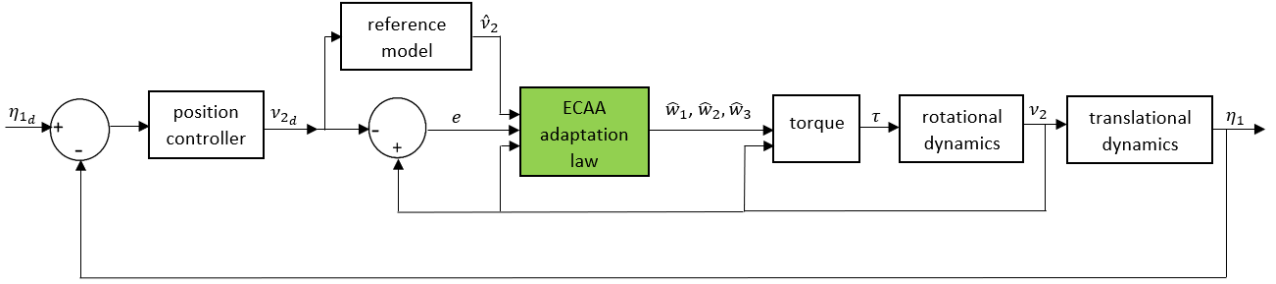
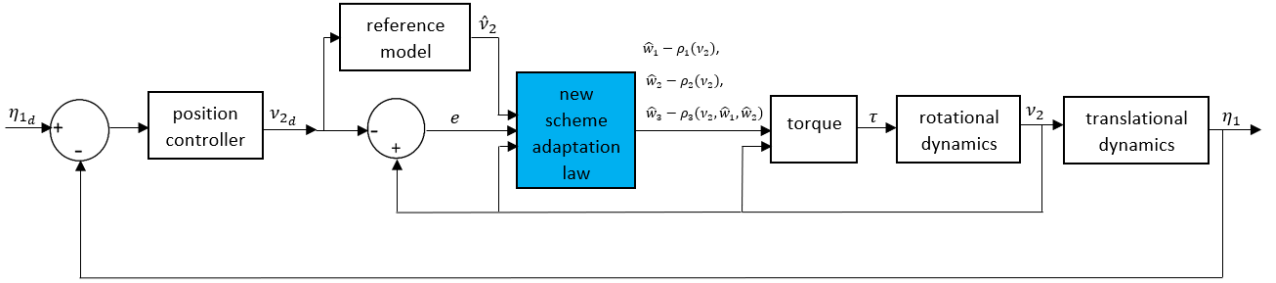FIGURE 1: The control system scheme of 6-DOF UAV based on Theorem 3.1.

FIGURE 2: The control system scheme of 6-DOF UAV based on Theorem 3.2.

$$
\begin{aligned}
&+ \hat{w}_1 f(\nu_2) + \hat{w}_2 \mathbf{1} \Big) \Big) + \mathrm{tr}\Big(\Gamma_1^{-1} \tilde{w}_1 \dot{\hat{w}}_1 \\
&+ \Gamma_2^{-1} \tilde{w}_2 \dot{\hat{w}}_2 + \Gamma_3^{-1} w_3 \tilde{w}_3 \dot{\hat{w}}_3 \Big) \\
&= -\tilde{\nu}_2^\mathsf{T} K_1 \tilde{\nu}_2 - \tilde{\nu}_2^\mathsf{T} K_2 \chi(\tilde{\nu}_2) + \tilde{\nu}_2^\mathsf{T} \\
&\quad \Big(-\tilde{w}_1 f(\nu_2) - \tilde{w}_2 \mathbf{1} + \sigma \mathbf{1} \\
&\quad - w_3 \tilde{w}_3 \big(K_1 e + K_2 \chi(\tilde{\nu}_2) + \hat{w}_1 f(\nu_2) \\
&\quad + \hat{w}_2 \mathbf{1} \big) \Big) + \mathrm{tr}\Big(\Gamma_1^{-1} \tilde{w}_1 \dot{\hat{w}}_1 + \Gamma_2^{-1} \tilde{w}_2 \dot{\hat{w}}_2 \\
&\quad + \Gamma_3^{-1} w_3 \tilde{w}_3 \dot{\hat{w}}_3 \Big) \\
&= -\tilde{\nu}_2^\mathsf{T} K_1 \tilde{\nu}_2 - \tilde{\nu}_2^\mathsf{T} K_2 \chi(\tilde{\nu}_2) + \tilde{\nu}_2^\mathsf{T} \sigma \mathbf{1} \\
&\quad + \mathrm{tr}\Big(\Gamma_1^{-1} \tilde{w}_1 \dot{\hat{w}}_1 + \Gamma_2^{-1} \tilde{w}_2 \dot{\hat{w}}_2 + \Gamma_3^{-1} w_3 \\
&\quad \tilde{w}_3 \dot{\hat{w}}_3 - \tilde{w}_1 F(\nu_2) \underline{\tilde{\nu}}_2 - \tilde{w}_2 \underline{\tilde{\nu}}_2 - w_3 \tilde{w}_3 \underline{\tilde{\nu}}_2 \\
&\quad \Big(K_1 E + K_2 \chi(\underline{\tilde{\nu}}_2) + \hat{w}_1 F(\nu_2) + \hat{w}_2 \Big) \\
&\leq -\tilde{\nu}_2^\mathsf{T} K_1 \tilde{\nu}_2 - \tilde{\nu}_2^\mathsf{T} K_2 \chi(\tilde{\nu}_2) + \frac{\alpha}{2} \tilde{\nu}_2^\mathsf{T} \tilde{\nu}_2 \\
&\quad + \frac{1}{2\alpha} \mathrm{tr}\Big(\mathrm{sgn}(|\underline{\tilde{\nu}}_2|) \sigma^2 \Big) \\
&\leq -\tilde{\nu}_2^\mathsf{T} (K_1 - \frac{\alpha}{2} I_3) \tilde{\nu}_2 \\
&\quad - \tilde{\nu}_2^\mathsf{T} (K_2 - \frac{1}{2\alpha} \delta^2) \chi(\tilde{\nu}_2) \\
&\leq -\tilde{\nu}_2^\mathsf{T} (K_1 - \frac{\alpha}{2} I_3) \tilde{\nu}_2 \leq 0,
\end{aligned}
$$

where $\alpha > 0$, $K_1 > \frac{\alpha}{2} I_3$ and $K_2 \geq \frac{1}{2\alpha} \delta^2$. From (27) and (30), we can see that $\dot{\tilde{\nu}}_2$, $\tilde{w}_1$, $\tilde{w}_2$, and $\tilde{w}_3$ are bounded. To show the tracking error $\tilde{\nu}_2$ is driven asymptotically to zero, we calculate the second time-derivative of Lyapunov function

$V(\tilde{\nu}_2, \tilde{w}_1, \tilde{w}_2, \tilde{w}_3)$ as

$$
\ddot{V}_{\tilde{\nu}_2 \tilde{w}_1 \tilde{w}_2 \tilde{w}_3} \leq -\tilde{\nu}_2^\mathsf{T} (2K_1 - \alpha I_3) \dot{\tilde{\nu}}_2. \tag{31}
$$

It shows from (30) that $\tilde{\nu}_2$ is uniformly bounded, and hence $\ddot{V}_{\tilde{\nu}_2 \tilde{w}_1 \tilde{w}_2 \tilde{w}_3}$ is bounded. This implies that $\dot{V}_{\tilde{\nu}_2 \tilde{w}_1 \tilde{w}_2 \tilde{w}_3}$ is uniformly continuous. By Barbalat's Lemma, one has $\lim_{t \to \infty} \tilde{\nu}_2(t) = 0$, it implies $\lim_{t \to \infty} e(t) = 0$. This completes the proof. ∎

It can be observed from the above formulation that the convergences of estimation errors $\tilde{w}_1$, $\tilde{w}_2$ and $\tilde{w}_3$ fully rely on $\tilde{\nu}_2(t)$. The values of $\mathrm{tr}(\tilde{w}_1 \dot{\hat{w}}_1)$, $\mathrm{tr}(\tilde{w}_2 \dot{\hat{w}}_2)$ and $\mathrm{tr}(\tilde{w}_3 \dot{\hat{w}}_3)$ are not always negative. Consequently, the adaptation law (27) will always update itself even the actual value of the unknown parameter is reached. In another side, it will stop updating itself if $\tilde{\nu}_2(t)$ converges to zero. It means that the tracking control is asymptotically achieved, even if the estimated parameters does not converge to the actual values. The controller (26) has a robust term $-K_2 \chi(\tilde{\nu}_2)$ to handle the perturbation term σ. The full control scheme of UAV using Theorem 3.1 is presented in Figure 1.

2) A new adaptive scheme

To compare and improve the ECAA scheme developed in the previous section, here we design a new adaptive control scheme to handle the uncertain parameters in the attitude dynamics of the UAV. Before presenting our new adaptive

approach, we define

$$
\begin{aligned}
z_1 &= \rho_1(\nu_2) - \hat{w}_1 + w_1 \\
z_2 &= \rho_2(\nu_2) - \hat{w}_2 + l \\
z_3 &= \rho_3(\nu_2, \hat{w}_1, \hat{w}_2) - \hat{w}_3 + w_3^{-1},
\end{aligned}
\tag{32}
$$

where

$$
\underline{\nu}_2 = \text{diag}(\nu_2), \ \underline{\tilde{\nu}}_2 = \text{diag}(\tilde{\nu}_2),
$$

and l is defined in Remark 2.1. The new approach is summarized in Theorem 3.2.

Theorem 3.2: (**New adaptive approach**) Consider the attitude dynamics (4), under Assumptions 1 and 2, the control law is designed as

$$
\tau = (\rho_3(\nu_2, \hat{w}_1, \hat{w}_2) - \hat{w}_3)(K_1 e + K_2 \chi(\tilde{\nu}_2) \\
- (\rho_1(\nu_2) - \hat{w}_1) f(\nu_2) - (\rho_2(\nu_2) - \hat{w}_2)\mathbf{1}),
\tag{33}
$$

where $\hat{w}_1$, $\hat{w}_2$ and $\hat{w}_3$ are adapted by the following update rules

$$
\begin{aligned}
\dot{\hat{w}}_1 &= \frac{\partial \rho_1(\nu_2)}{\partial \nu_2}(-K_1 E - K_2 \chi(\underline{\tilde{\nu}}_2)), \\
\dot{\hat{w}}_2 &= \frac{\partial \rho_2(\nu_2)}{\partial \nu_2}(-K_1 E - K_2 \chi(\underline{\tilde{\nu}}_2)), \\
\dot{\hat{w}}_3 &= \frac{\partial \rho_3(\nu_2, \hat{w}_1, \hat{w}_2)}{\partial \nu_2}(-K_1 E - K_2 \chi(\underline{\tilde{\nu}}_2)) \\
&\quad + \frac{\partial \rho_3(\nu_2, \hat{w}_1, \hat{w}_2)}{\partial \hat{w}_1}\dot{\hat{w}}_1 + \frac{\partial \rho_3(\nu_2, \hat{w}_1, \hat{w}_2)}{\partial \hat{w}_2}\dot{\hat{w}}_2,
\end{aligned}
\tag{34}
$$

for some selection of $\Lambda_1, \Lambda_2, \Lambda_3 > 0$, $\alpha \geq \frac{1}{2}$, $K_1 > \alpha I_3$, $K_2 \geq \frac{1}{2\alpha}\delta^2$; and $\rho_1(\nu_2)$, $\rho_2(\nu_2)$ and $\rho_3(\nu_2)$ are

$$
\begin{aligned}
\rho_1(\nu_2) &= -\Lambda_1 F(\nu_2)\underline{\nu}_2, \\
\rho_2(\nu_2) &= -\Lambda_2 \underline{\nu}_2, \\
\rho_3(\nu_2, \hat{w}_1, \hat{w}_2) &= -\Lambda_3 \underline{\nu}_2 (K_1 E + K_2 \chi(\underline{\tilde{\nu}}_2) - (\rho_1(\nu_2) \\
&\quad - \hat{w}_1) F(\nu_2) - \rho_2(\nu_2) + \hat{w}_2),
\end{aligned}
\tag{35}
$$

then the time-derivative of

$$
V_{\tilde{\nu}_2 z_1 z_2 z_3} = \frac{1}{2}\tilde{\nu}_2^\intercal \tilde{\nu}_2 + \text{tr}\left(\frac{1}{2}\Lambda_1^{-1} z_1^2 + \frac{1}{2}\Lambda_2^{-1} z_2^2 \\
+ \frac{1}{2}\Lambda_3^{-1} w_3 z_3^2\right),
\tag{36}
$$

along the closed-loop system (4)+(33)+(34) is

$$
\dot{V}_{\tilde{\nu}_2 z_1 z_2 z_3} \leq -\tilde{\nu}_2^\intercal (K_1 - \alpha I_3)\tilde{\nu}_2 \leq 0.
\tag{37}
$$

Proof: The error dynamic of the closed-loop system (4)+(33)+(34) can be written as

$$
\begin{aligned}
\dot{\nu}_2 &= K_1(\hat{\nu}_2 - \nu_{2_d}) + w_1 f(\nu_2) + w_2 \mathbf{1} + w_3 \\
&\quad (\rho_3(\nu_2, \hat{w}_1, \hat{w}_2) - \hat{w}_3)(K_1 e + K_2 \chi(\tilde{\nu}_2) \\
&\quad - (\rho_1(\nu_2) - \hat{w}_1) f(\nu_2) - (\rho_2(\nu_2) - \hat{w}_2)\mathbf{1}) \\
&= K_1(\hat{\nu}_2 - \nu_{2_d}) + w_1 f(\nu_2) + w_2 \mathbf{1} + w_3 \\
&\quad (z_3 - w_3^{-1})(K_1 e + K_2 \chi(\tilde{\nu}_2) - (\rho_1(\nu_2) - \hat{w}_1) \\
&\quad f(\nu_2) - (\rho_2(\nu_2) - \hat{w}_2)\mathbf{1}) \\
&= K_1(\hat{\nu}_2 - \nu_{2_d}) + w_1 f(\nu_2) + w_2 \mathbf{1} + w_3 z_3 \\
&\quad (K_1 e + K_2 \chi(\tilde{\nu}_2) - (\rho_1(\nu_2) - \hat{w}_1) f(\nu_2) \\
&\quad - (\rho_2(\nu_2) - \hat{w}_2)\mathbf{1}) - K_1 e - K_2 \chi(\tilde{\nu}_2) \\
&\quad + (\rho_1(\nu_2) - \hat{w}_1) f(\nu_2) + (\rho_2(\nu_2) - \hat{w}_2)\mathbf{1} \\
&= -K_1 \tilde{\nu}_2 - K_2 \chi(\tilde{\nu}_2) + z_1 f(\nu_2) + (z_2 + \sigma)\mathbf{1} \\
&\quad + w_3 z_3 (K_1 e + K_2 \chi(\tilde{\nu}_2) - (\rho_1(\nu_2) - \hat{w}_1) \\
&\quad f(\nu_2) - (\rho_2(\nu_2) - \hat{w}_2)\mathbf{1}).
\end{aligned}
\tag{38}
$$

For convenience of presentation, we rewrite the Lyapunov function (36) as follows

$$
V_{\tilde{\nu}_2 z_1 z_2 z_3} = V_{\tilde{\nu}_2} + V_{z_1} + V_{z_2} + V_{z_3},
\tag{39}
$$

where

$$
\begin{aligned}
V_{\tilde{\nu}_2} &= \frac{1}{2}\tilde{\nu}_2^\intercal \tilde{\nu}_2, \ V_{z_1} = \text{tr}\left(\frac{1}{2}\Lambda_1^{-1} z_1^2\right), \\
V_{z_2} &= \text{tr}\left(\frac{1}{2}\Lambda_2^{-1} z_2^2\right), \ V_{z_3} = \text{tr}\left(\frac{1}{2}\Lambda_3^{-1} w_3 z_3^2\right).
\end{aligned}
$$

Direct calculation shows that the time-derivative of $V_{\tilde{\nu}_2}$ along the dynamics (38) is

$$
\begin{aligned}
\dot{V}_{\tilde{\nu}_2} &= \tilde{\nu}_2^\intercal \dot{\tilde{\nu}}_2 \\
&= \tilde{\nu}_2^\intercal \Big(-K_1 \tilde{\nu}_2 - K_2 \chi(\tilde{\nu}_2) + z_1 f(\nu_2) + (z_2 + \sigma)\mathbf{1} \\
&\quad + w_3 z_3 (K_1 e + K_2 \chi(\tilde{\nu}_2) - (\rho_1(\nu_2) - \hat{w}_1) \\
&\quad f(\nu_2) - (\rho_2(\nu_2) - \hat{w}_2)\mathbf{1}) \Big) \\
&= -\tilde{\nu}_2^\intercal K_1 \tilde{\nu}_2 - \tilde{\nu}_2^\intercal K_2 \chi(\tilde{\nu}_2) + \tilde{\nu}_2^\intercal \Big(z_1 f(\nu_2) \\
&\quad + (z_2 + \sigma)\mathbf{1} + w_3 z_3 (K_1 e + K_2 \chi(\tilde{\nu}_2) \\
&\quad - (\rho_1(\nu_2) - \hat{w}_1) f(\nu_2) - (\rho_2(\nu_2) - \hat{w}_2)\mathbf{1}) \Big) \\
&\leq -\tilde{\nu}_2^\intercal (K_1 - \alpha I_3)\tilde{\nu}_2 - \tilde{\nu}_2^\intercal K_2 \chi(\tilde{\nu}_2) + \frac{1}{2\alpha}\Big(z_1 \\
&\quad f(\nu_2) + z_2 \mathbf{1} + w_3 z_3 (K_1 e + K_2 \chi(\tilde{\nu}_2) \\
&\quad - (\rho_1(\nu_2) - \hat{w}_1) f(\nu_2) - (\rho_2(\nu_2) - \hat{w}_2)\mathbf{1}) \Big)^\intercal \\
&\quad \text{sgn}(|\tilde{\nu}_2|)\Big(z_1 f(\nu_2) + z_2 \mathbf{1} + w_3 z_3 (K_1 e \\
&\quad + K_2 \chi(\tilde{\nu}_2) - (\rho_1(\nu_2) - \hat{w}_1) f(\nu_2) - (\rho_2(\nu_2) \\
&\quad - \hat{w}_2)\mathbf{1}) \Big) + \frac{1}{2\alpha}\Big(z_1 f(\nu_2) + z_2 \mathbf{1} + w_3 z_3 (K_1 e \\
&\quad + K_2 \chi(\tilde{\nu}_2) - (\rho_1(\nu_2) - \hat{w}_1) f(\nu_2) - (\rho_2(\nu_2) \\
&\quad - \hat{w}_2)\mathbf{1}) \Big)^\intercal \sigma \text{sgn}(|\tilde{\nu}_2|)\Big(z_1 f(\nu_2) + z_2 \mathbf{1} + w_3 z_3 \\
&\quad (K_1 e + K_2 \chi(\tilde{\nu}_2) - (\rho_1(\nu_2) - \hat{w}_1) f(\nu_2)
\end{aligned}
$$

$$- (\rho_2(\nu_2) - \hat{w}_2)\mathbf{1}\big)\big) + \frac{1}{2\alpha}\mathbf{1}^\top\sigma^2\mathbf{1}$$

$$\leq -\tilde{\nu}_2^\top(K_1 - \alpha I_3)\tilde{\nu}_2 - \tilde{\nu}_2^\top K_2\chi(\tilde{\nu}_2) + \frac{1}{2\alpha}$$

$$\mathrm{tr}\Big(\mathrm{sgn}(|\tilde{\underline{\nu}}_2|)\big(z_1 F(\nu_2) + z_2 + w_3 z_3\big(K_1 E$$

$$+ K_2\chi(\tilde{\underline{\nu}}_2) - (\rho_1(\nu_2) - \hat{w}_1)F(\nu_2) - \rho_2(\nu_2)$$

$$+ \hat{w}_2\big)\big)^2\big(\sigma + I_3\big)\Big) + \frac{1}{2\alpha}\big(\mathrm{sgn}(|\tilde{\underline{\nu}}_2|)\sigma^2\big). \tag{40}$$

We can rewrite the dynamics (4) under controller (33) as follows

$$\dot{\nu}_2 = w_1 f(\nu_2) + w_2\mathbf{1} + w_3\tau$$

$$= w_1 f(\nu_2) + w_2\mathbf{1} + w_3(\rho_3(\nu_2, \hat{w}_1, \hat{w}_2) - \hat{w}_3)$$

$$\big(K_1 e + K_2\chi(\tilde{\nu}_2) - (\rho_1(\nu_2) - \hat{w}_1)f(\nu_2)$$

$$- (\rho_2(\nu_2) - \hat{w}_2)\mathbf{1}\big)$$

$$= w_1 f(\nu_2) + w_2\mathbf{1} + w_3(z_3 - w_3^{-1})\big(K_1 e + K_2$$

$$\chi(\tilde{\nu}_2) - (\rho_1(\nu_2) - \hat{w}_1)f(\nu_2) - (\rho_2(\nu_2) - \hat{w}_2)\mathbf{1}\big)$$

$$= w_1 f(\nu_2) + w_2\mathbf{1} + w_3 z_3\big(K_1 e + K_2\chi(\tilde{\nu}_2)$$

$$- (\rho_1(\nu_2) - \hat{w}_1)f(\nu_2) - (\rho_2(\nu_2) - \hat{w}_2)\mathbf{1}\big)$$

$$- K_1 e - K_2\chi(\tilde{\nu}_2) + (\rho_1(\nu_2) - \hat{w}_1)f(\nu_2)$$

$$+ (\rho_2(\nu_2) - \hat{w}_2)\mathbf{1}$$

$$= -K_1 e - K_2\chi(\tilde{\nu}_2) + z_1 f(\nu_2) + (z_2 + \sigma)\mathbf{1}$$

$$+ w_3 z_3\big(K_1 e + K_2\chi(\tilde{\nu}_2) - (\rho_1(\nu_2) - \hat{w}_1)$$

$$f(\nu_2) - (\rho_2(\nu_2) - \hat{w}_2)\mathbf{1}\big),$$

thus

$$\dot{\underline{\nu}}_2 = -K_1 E - K_2\chi(\tilde{\underline{\nu}}_2) + z_1 F(\nu_2) + z_2 + \sigma$$

$$+ w_3 z_3\big(K_1 E + K_2\chi(\tilde{\underline{\nu}}_2) - (\rho_1(\nu_2) - \hat{w}_1)$$

$$F(\nu_2) - \rho_2(\nu_2) + \hat{w}_2\big).$$

The time-derivative of V_{z_1}, V_{z_2} and V_{z_3} is calculated as follows

$$\dot{V}_{z_1} = \mathrm{tr}\Big(\Lambda_1^{-1}z_1\dot{z}_1\Big)$$

$$= \mathrm{tr}\Big(\Lambda_1^{-1}z_1\Big(\frac{\partial\rho_1(\nu_2)}{\partial\nu_2}\dot{\underline{\nu}}_2 - \dot{\hat{w}}_1\Big)\Big)$$

$$= \mathrm{tr}\Big(\Lambda_1^{-1}z_1\Big(\frac{\partial\rho_1(\nu_2)}{\partial\nu_2}\big(-K_1 E - K_2\chi(\tilde{\underline{\nu}}_2)$$

$$+ z_1 F(\nu_2) + z_2 + \sigma + w_3 z_3\big(K_1 E + K_2$$

$$\chi(\tilde{\underline{\nu}}_2) - (\rho_1(\nu_2) - \hat{w}_1)F(\nu_2) - \rho_2(\nu_2) + \hat{w}_2\big)\big)$$

$$- \dot{\hat{w}}_1\Big)\Big)$$

$$= -\mathrm{tr}\Big(z_1 F(\nu_2)\mathrm{sgn}(|\tilde{\underline{\nu}}_2|)\big(z_1 F(\nu_2) + z_2 + \sigma$$

$$+ w_3 z_3\big(K_1 E + K_2\chi(\tilde{\underline{\nu}}_2) - (\rho_1(\nu_2) - \hat{w}_1)$$

$$F(\nu_2) - \rho_2(\nu_2) + \hat{w}_2\big)\big)\Big), \tag{41}$$

$$\dot{V}_{z_2} = \mathrm{tr}\Big(\Lambda_2^{-1}z_2\dot{z}_2\Big)$$

$$= \mathrm{tr}\Big(\Lambda_2^{-1}z_2\Big(\frac{\partial\rho_2(\nu_2)}{\partial\nu_2}\dot{\underline{\nu}}_2 - \dot{\hat{w}}_2\Big)\Big)$$

$$= \mathrm{tr}\Big(\Lambda_2^{-1}z_2\Big(\frac{\partial\rho_2(\nu_2)}{\partial\nu_2}\big(-K_1 E - K_2\chi(\tilde{\underline{\nu}}_2)$$

$$+ z_1 F(\nu_2) + z_2 + \sigma + w_3 z_3\big(K_1 E + K_2\chi(\tilde{\underline{\nu}}_2)$$

$$- (\rho_1(\nu_2) - \hat{w}_1)F(\nu_2) - \rho_2(\nu_2) + \hat{w}_2\big)\big) - \dot{\hat{w}}_2\Big)\Big)$$

$$= -\mathrm{tr}\Big(z_2\mathrm{sgn}(|\tilde{\underline{\nu}}_2|)\big(z_1 F(\nu_2) + z_2 + \sigma + w_3 z_3$$

$$\big(K_1 E + K_2\chi(\tilde{\underline{\nu}}_2) - (\rho_1(\nu_2) - \hat{w}_1)F(\nu_2)$$

$$- \rho_2(\nu_2) + \hat{w}_2\big)\big)\Big), \tag{42}$$

$$\dot{V}_{z_3} = \mathrm{tr}\Big(\Lambda_3^{-1}w_3 z_3\dot{z}_3\Big)$$

$$= \mathrm{tr}\Big(\Lambda_3^{-1}w_3 z_3\Big(\frac{\partial\rho_3(\nu_2, \hat{w}_1, \hat{w}_2)}{\partial\nu_2}\dot{\underline{\nu}}_2$$

$$+ \frac{\partial\rho_3(\nu_2, \hat{w}_1, \hat{w}_2)}{\partial\hat{w}_1}\dot{\hat{w}}_1 + \frac{\partial\rho_3(\nu_2, \hat{w}_1, \hat{w}_2)}{\partial\hat{w}_2}\dot{\hat{w}}_2$$

$$- \dot{\hat{w}}_3\Big)\Big)$$

$$= \mathrm{tr}\Big(\Lambda_3^{-1}w_3 z_3\Big(\frac{\partial\rho_3(\nu_2, \hat{w}_1, \hat{w}_2)}{\partial\nu_2}\big(-K_1 E$$

$$- K_2\chi(\tilde{\underline{\nu}}_2) + z_1 F(\nu_2) + z_2 + \sigma$$

$$+ w_3 z_3\big(K_1 E + K_2\chi(\tilde{\underline{\nu}}_2) - (\rho_1(\nu_2) - \hat{w}_1)$$

$$F(\nu_2) - \rho_2(\nu_2) + \hat{w}_2\big)\big) - \dot{\hat{w}}_3$$

$$+ \frac{\partial\rho_3(\nu_2, \hat{w}_1, \hat{w}_2)}{\partial\hat{w}_1}\dot{\hat{w}}_1 + \frac{\partial\rho_3(\nu_2, \hat{w}_1, \hat{w}_2)}{\partial\hat{w}_2}\dot{\hat{w}}_2\Big)\Big)$$

$$= -\mathrm{tr}\Big(\mathrm{sgn}(|\tilde{\underline{\nu}}_2|)w_3 z_3\big(K_1 E + K_2\chi(\tilde{\underline{\nu}}_2)$$

$$- (\rho_1(\nu_2) - \hat{w}_1)F(\nu_2) - \rho_2(\nu_2) + \hat{w}_2\big)\big(z_1 F(\nu_2)$$

$$+ z_2 + \sigma + w_3 z_3\big(K_1 E + K_2\chi(\tilde{\underline{\nu}}_2) - (\rho_1(\nu_2)$$

$$- \hat{w}_1)F(\nu_2) - \rho_2(\nu_2) + \hat{w}_2\big)\big)\Big). \tag{43}$$

From (40)+(41)+(42)+(43), we can calculate the time-derivative of $V_{\tilde{\nu}_2 z_1 z_2 z_3}$ as follows

$$\dot{V}_{\tilde{\nu}_2 z_1 z_2 z_3} \leq -\tilde{\nu}_2^\top(K_1 - \alpha I_3)\tilde{\nu}_2 - \tilde{\nu}_2^\top K_2\chi(\tilde{\nu}_2) + \frac{1}{2\alpha}$$

$$\mathrm{tr}\Big(\mathrm{sgn}(|\tilde{\underline{\nu}}_2|)\big(z_1 F(\nu_2) + z_2 + w_3 z_3\big(K_1 E$$

$$+ K_2\chi(\tilde{\underline{\nu}}_2) - (\rho_1(\nu_2) - \hat{w}_1)F(\nu_2) - \rho_2(\nu_2)$$

$$+ \hat{w}_2\big)\big)^2\big(\sigma + I_3\big)\Big) + \frac{1}{2\alpha}\big(\mathrm{sgn}(|\tilde{\underline{\nu}}_2|)\sigma^2\big)$$

$$- \mathrm{tr}\Big(\mathrm{sgn}(|\tilde{\underline{\nu}}_2|)\big(z_1 F(\nu_2) + z_2 + w_3 z_3\big(K_1 E$$

$$+ K_2\chi(\tilde{\underline{\nu}}_2) - (\rho_1(\nu_2) - \hat{w}_1)F(\nu_2) - \rho_2(\nu_2)$$

$$+ \hat{w}_2\big)\big)^2\big(\sigma + I_3\big)\Big)$$

$$\leq -\tilde{\nu}_2^\top(K_1 - \alpha I_3)\tilde{\nu}_2 - \tilde{\nu}_2^\top(K_2 - \frac{1}{2\alpha}\delta^2)\chi(\tilde{\nu}_2)$$

$$- \frac{2\alpha - 1}{2\alpha}\mathrm{tr}\Big(\mathrm{sgn}(|\tilde{\underline{\nu}}_2|)\big(z_1 F(\nu_2) + z_2$$

$$+ w_3 z_3\big(K_1 E + K_2\chi(\tilde{\underline{\nu}}_2) - (\rho_1(\nu_2) - \hat{w}_1)$$

$$F(\nu_2) - \rho_2(\nu_2) + \hat{w}_2\big)\big)^2\big(\sigma + I_3\big)\Big) \tag{44}$$

By selecting $\alpha \geq \frac{1}{2}$, $K_1 > \alpha I_3$, and $K_2 \geq \frac{1}{2\alpha}\delta^2$, then $\dot{V}_{\tilde{\nu}_2 z_1 z_2 z_3} \leq -\tilde{\nu}_2^\top(K_1 - \alpha I_3)\tilde{\nu}_2 \leq 0$. The proof is thus completed. ∎

Similar to the ECAA developed in Theorem 3.1, the tracking control can be asymptotically achieved without the need for convergence of $\hat{w}_1$, $\hat{w}_2$ and $\hat{w}_3$ to the actual values of w_1, w_2 and w_3. The controller (33) also has a robust term $-K_2\chi(\tilde{\nu}_2)$ to handle perturbation σ. The adaptive approach in Theorem 3.2 has an additional continuous function $\rho_1(\nu_2)$, $\rho_2(\nu_2)$ and $\rho_3(\nu_2, \hat{w}_1, \hat{w}_2)$ to assist in estimating the parameters $\hat{w}_1$, $\hat{w}_2$ and $\hat{w}_3$ and handling the parametric uncertainties. The schematic block diagram of the adaptive control scheme proposed in Theorem 3.2 is illustrated in Figure 2.

Remark 3.1: In Theorems 3.1 and 3.2, the unknown vectors w_1 and w_3 are in the class of piecewise constant functions. However, treating them as constant parameters will not put any harms to the proof. In fact, the value of the parameters during the switching times can be modeled as a sign function with a bounded amplitude and this reflects itself as a bounded additive disturbance, similar to w_2, in the dynamic model of the system in (4). This is true since the propeller motors work as a low-pass filter and this prevents a sudden jump in the response of the system. Also, since the motor torques are bounded in practice, the effect of jumps can be modeled as a bounded disturbance added to the weight w_2. Therefore, the effect of this disturbance can be cancelled by proper tuning of K_2 gain in (29) for the ECAA and (44) for the new adaptive scheme to ensure the stability of the closed-loop system during the switching times.

IV. SIMULATION RESULTS

The performance of the proposed approaches is evaluated through numerical analysis in this section. The nested controller is implemented numerically by proposing a PD controller as the translational controller. The parameters tuned for the PD controller in Section III-A are $K_P = K_D = 10I_3$. The attitude controller is designed according to the Theorem 3.1 and 3.2. The gains tuned for the control law (26) and adaptive law (27) are

$$
\begin{aligned}
K_1 &= \mathrm{diag}\begin{bmatrix} 900 & 1200 & 1500 \end{bmatrix}, \\
K_2 &= 10^{-3}\mathrm{diag}\begin{bmatrix} 0.1333 & 0.4 & 0.02 \end{bmatrix}, \\
\Lambda_1 &= 100I_3, \ \Lambda_2 = 10I_3, \ \Lambda_3 = 100I_3.
\end{aligned} \tag{45}
$$

While the gains tuned for the control law (33) and adaptive law (34) are

$$
\begin{aligned}
K_1 &= \mathrm{diag}\begin{bmatrix} 900 & 1200 & 1500 \end{bmatrix}, \\
K_2 &= 10^{-3}\mathrm{diag}\begin{bmatrix} 0.1333 & 0.4 & 0.02 \end{bmatrix}, \\
\Gamma_1 &= 5I_3, \ \Gamma_2 = 0.1I_3, \ \Gamma_3 = 10^{-3}I_3.
\end{aligned} \tag{46}
$$

The parameters of the quadrotor UAV used for the simulation and numerical analysis are listed in Table 1.

TABLE 1: The parameters of the UAV.

Parameter name	Notation	Value
Mass	m	$2.4kg$
Gravity acceleration	g	$9.8m/s^2$
Translational drag coefficient	k_t	0.95
Inertia of x-axis	I_x	$0.16kg.m^2$
Inertia of y-axis	I_y	$0.16kg.m^2$
Inertia of z-axis	I_z	$0.32kg.m^2$

Moreover, the following time-varying external disturbance $w_2 = \mathrm{diag}\begin{bmatrix} 0.1\sin(t) & 0.4\cos(t) & 0.2\sin(t) \end{bmatrix}^\top$ is added to the attitude dynamics. The inertia parameters are assumed to be time-varying piecewise constant functions, where the value of the parameters is increased by 50% at $t \geq 4s$.

The simulation results using ECAA and the new approach are depicted in Figures 3-11. We also presented the performance of the adaptive sliding mode control (ASMC) [10] for the comparative study. As can be seen from these figures, both translational and rotational states of the quadrotor can follow the desired trajectories, verifying the results proven in Theorems 3.1 and 3.2. Figure 3 illustrates the performance of (27) and (34) to handle uncertainties in the rotational dynamics. We can see that our new scheme has better performance to maintain the rotational motions while the gains of ECAA are higher than our new scheme. The mismatch between the actual states and the desired trajectories can be seen in Figure 7.

For the convenience of presentation, we calculate the fitness of the states using the following formula

$$
\mathrm{fitness}(\%) = 100\Big(1 - \frac{\|\text{desired trajectory} - \text{state}\|}{\|\text{desired trajectory} - E(\text{state})\|}\Big), \tag{47}
$$

where $E(\text{state})$ refers to the mean of state.

The fitness of the steady state error trajectories using ECAA and the new approach from $t = 0.1s$ to $t = 7s$ are presented in Table 2. It is evident from the simulation results that our new approach shows better performance compared to ECAA.

TABLE 2: The fitness values of the UAV rotational states.

Variable	ASMC	ECAA	New scheme
p	98.8427%	99.4601%	98.9904%
q	96.7089%	98.4171%	98.6254%
r	94.3836%	94.3892%	96.4960%
average	96.6451%	97.4221%	98.0373%

The profile of τ using ECAA and the new approaches can be seen in Figures 6. The total effort of torque τ is presented in Table 3. We can see that the total control effort of τ in our new scheme is almost half of the ECAA approach.

TABLE 3: The torque efforts of the proposed controllers.

Variable	ASMC	ECAA	New scheme
total effort of τ_p	3.0323×10^4	8.6303	8.2457
total effort of τ_q	4.5003×10^4	1.0896×10^3	449.8616
total effort of τ_r	17.4044	7.0189	7.0709
total	7.5374×10^4	1.1052×10^3	496.0806

The numerical results based on both adaptive schemes proposed in Theorem 3.1 and 3.2 are plotted in Figure 9-11. Each scheme has a robust term that can be adjusted by tunning K_2 to handle the perturbation σ. As a result, each estimated parameter is not necessarily converging to its actual value. More scenarios are simulated by increasing the external disturbance w_2 by 50% and reduce the control gains of the adaptive schemes. The new gains for ECAA are

$$
\begin{aligned}
&K_P = 7I_3, \ K_D = 7I_3, \\
&K_1 = \mathrm{diag} \begin{bmatrix} 675 & 900 & 1125 \end{bmatrix}, \\
&K_2 = 10^{-3}\mathrm{diag} \begin{bmatrix} 0.4 & 1.2 & 0.1 \end{bmatrix}, \\
&\Lambda_1 = 70I_3, \ \Lambda_2 = 6I_3, \ \Lambda_3 = 80I_3,
\end{aligned} \tag{48}
$$

while the new gains of new scheme are tuned as follows

$$
\begin{aligned}
&K_P = 7I_3, \ K_D = 7I_3, \\
&K_1 = \mathrm{diag} \begin{bmatrix} 675 & 900 & 1125 \end{bmatrix}, \\
&K_2 = 10^{-3}\mathrm{diag} \begin{bmatrix} 0.4 & 1.2 & 0.1 \end{bmatrix}, \\
&\Gamma_1 = 3I_3, \ \Gamma_2 = 0.08I_3, \ \Gamma_3 = 8 \times 10^{-4}I_3.
\end{aligned} \tag{49}
$$

The results show that our controllers are able to maintain UAV to follow the desired trajectory. Similar to the previous scenario, the new scheme has a better performance to tackle the tracking control problem. The fitness of the steady state trajectories for both scenarios, calculated from $t = 0.1s$ to $t = 7s$ can be seen in Table 4. Also, the total effort of torque τ is presented in Table 5. The effect of the initial conditions on the performance of the system is investigated using three different initial conditions presented in (50). Similar to the previous scenario, both ECAA and the new adaptive approach are able to maintain the attitude motions as illustrated in Figure 12.

$$
\begin{aligned}
&\text{Initial Condition 1} \Rightarrow \nu_2(0) = \begin{bmatrix} 0.12 & -1 & 0.003 \end{bmatrix}^\mathsf{T}, \\
&\text{Initial Condition 2} \Rightarrow \nu_2(0) = \begin{bmatrix} 0.06 & -0.5 & 0.0015 \end{bmatrix}^\mathsf{T}, \\
&\text{Initial Condition 3} \Rightarrow \nu_2(0) = \begin{bmatrix} -0.05 & 1 & -0.004 \end{bmatrix}^\mathsf{T}.
\end{aligned} \tag{50}
$$

TABLE 4: The fitness values of the UAV rotational states when w_2 is increased by 50%.

Variable	ECAA	New scheme
p	99.2983%	97.7358%
q	98.1818%	98.5850%
r	91.5158%	93.0648%
average	96.3319%	96.4619%

TABLE 5: The torque efforts of the proposed controllers when w_2 is increased by 50%.

Variable	ECAA	New scheme
total effort of τ_p	42.8333	9.9299
total effort of τ_q	1.6363×10^4	1.8858×10^3
total effort of τ_r	7.0358	7.7456
total	1.6413×10^4	1.9344×10^3

From the above simulations, it can be inferred that our proposed controllers have less computational complexity compared to the adaptive intelligent controllers using techniques such as fuzzy, genetic algorithms, and neural networks. Therefore, this provides more opportunity for practical implementation of the algorithms in real-time resource constraint applications such as UAVs.

V. CONCLUSION AND DIRECTIONS FOR FUTURE WORK

This paper presents a fully tracking control for 6-DOF of UAV with uncertain parameters. The tracking position control is designed using a virtual PD controller. Two adaptive approaches are proposed for tracking control of attitude dynamics with uncertain time-varying parameters. All parameters in the attitude dynamics are unknown for feedback control design. An external time-varying disturbance is also added to the dynamical system. In the beginning, ECAA scheme is proposed to handle the uncertainties in the dynamics. To improve the performance of the classical scheme, we develop a new adaptive approach by adding a continuous function to the control structure. Both schemes contain a robust term to handle the perturbation caused by the unknown time-varying parameters. To verify and compare our approaches, we conduct several simulations under various settings for a UAV. It will be interesting to extend this scheme for more complicated dynamics such as for multiple heterogeneous UAV with uncertainties. Also, it will be interesting to apply the current scheme to a quadrotor UAV.

REFERENCES

[1] Brian DO Anderson et al. Failures of adaptive control theory and their resolution. *Communications in Information & Systems*, 5(1):1–20, 2005.

[2] Alessandro Astolfi, Dimitrios Karagiannis, and Romeo Ortega. *Nonlinear and adaptive control with applications*. Springer Science & Business Media, 2007.

[3] Thomas Burrell, Craig West, Stephens D Monk, Allahyar Montezeri, and C James Taylor. Towards a cooperative robotic system for autonomous pipe cutting in nuclear decommissioning. In *2018 UKACC 12th International Conference on Control (CONTROL)*, pages 283–288. IEEE, 2018.

[4] Aydin Can, H. Efstathiades, , and Allahyar Montazeri. Robust nested nonlinear position control of a quadrotor platform in a 3d space. In *2020 International Conference on Nonlinearity, Information and Robotics*, 2020.

[5] Kaiwen Chen and Alessandro Astolfi. I&I adaptive control for systems with varying parameters. In *2018 IEEE Conference on Decision and Control (CDC)*, pages 2205–2210. IEEE, 2018.

[6] A. Das and F. Lewis. Distributed adaptive control for synchronization of unknown nonlinear networked systems. *Automatica*, 46(12):2014–2021, 2010.

[7] A. Das and F. Lewis. Cooperative adaptive control for synchronization of second-order systems with unknown
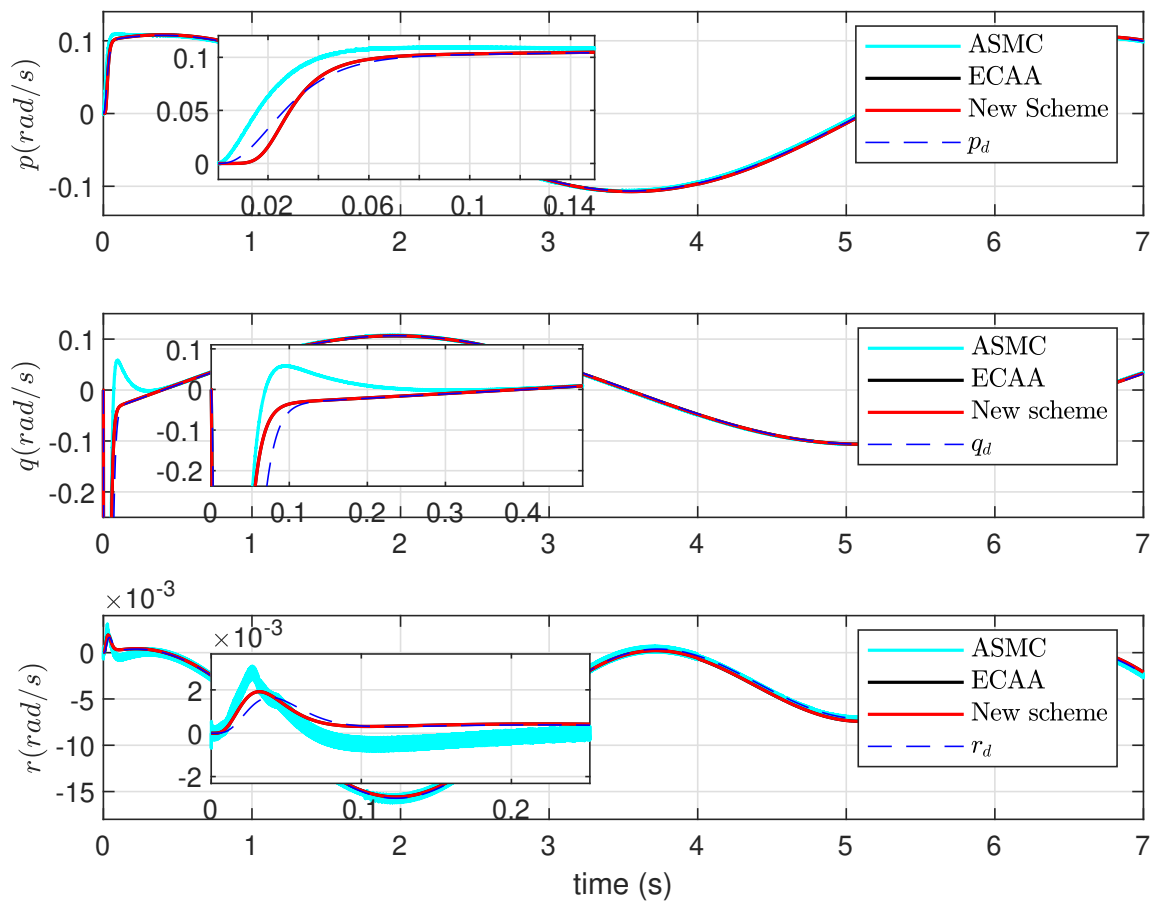
FIGURE 3: Profile of p, q and r.

nonlinearites. *International Journal of Robust and Nonlinear Control*, 21(13):1509–1524, 2011.

[8] Sami El-Ferik, Basem Almadani, and Siddig Mustafa Elkhider. Formation control of multi unmanned aerial vehicle systems based on dds middleware. *IEEE Access*, 8:44211–44218, 2020.

[9] Naira Hovakimyan and Chengyu Cao. *L1 adaptive control theory: guaranteed robustness with fast adaptation*, volume 21. SIAM-Society for Industrial and Applied Mathematics, 2010.

[10] Tianpeng Huang, Deqing Huang, Zhikai Wang, and Awais Shah. Robust tracking control of a quadrotor uav based on adaptive sliding mode controller. *Complexity*, 2019.

[11] Imil Hamda Imran. Cooperative control of heterogeneous systems based on immersion and invariance adaptive control. Master's thesis, King Fahd University of Petroleum and Minerals, KSA, 2015.

[12] Imil Hamda Imran and Allahyar Montazeri. An adaptive scheme to estimate unknown parameters of an unmanned aerial vehicle. In *2020 International Confer-ence on Nonlinearity, Information and Robotics*, 2020.

[13] Imil Hamda Imran and Allahyar Montazeri. Adaptive closed-loop identification and tracking control of an aerial vehicle with unknown inertia parameters. *IFAC-PapersOnLine*, 2021.

[14] Imil Hamda Imran, Zhiyong Chen, Yamin Yan, and Minyue Fu. Adaptive consensus of nonlinearly parameterized multi-agent systems. *IEEE Control Systems Letters*, 3(3):505–510, 2019.

[15] Imil Hamda Imran, Zhiyong Chen, Lijun Zhu, and Minyue Fu. A distributed adaptive scheme for multi-agent systems. *Asian Journal of Control*, 2020.

[16] Arief Barkah Koesdwiady. Immersion and invariance control design for unmanned aerial vehicle. Master's thesis, King Fahd University of Petroleum and Minerals (Saudi Arabia), 2013.

[17] Shushuai Li, Yaonan Wang, Jianhao Tan, and Yan Zheng. Adaptive rbfnns/integral sliding mode control for a quadrotor aircraft. *Neurocomputing*, 216:126–134, 2016.

[18] Xiangbin Liu, Romeo Ortega, Hongye Su, and Jian
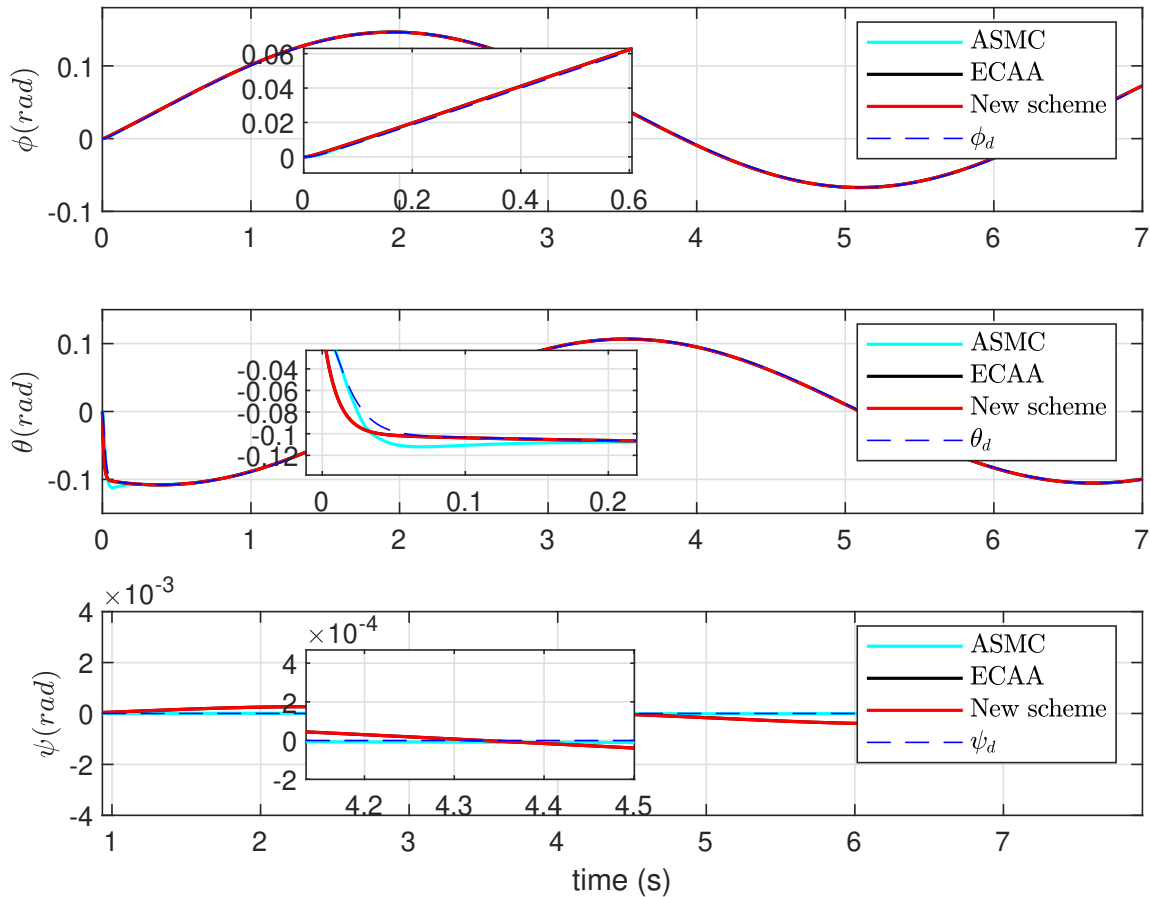
FIGURE 4: Profile of ϕ, θ and ψ.

Chu. Immersion and invariance adaptive control of nonlinearly parameterized nonlinear systems. *IEEE Transactions on Automatic Control*, 55(9):2209–2214, 2010.

[19] Allahyar Montazeri, Craig West, Stephen David Monk, and C James Taylor. Dynamic modelling and parameter estimation of a hydraulic robot manipulator using a multi-objective genetic algorithm. *International Journal of Control*, 90(4):661–683, 2017.

[20] Allahyar Montazeri, Aydin Can, and Imil Hamda Imran. Unmanned aerial systems: Autonomy, cognition and control. In *Unmanned aerial systems: theoretical foundation and applications*. Elsevier, 2020.

[21] Kumpati S Narendra and Anuradha M Annaswamy. *Stable adaptive systems*. Prentice Hall: Englewood Cliffs. NJ, 1989.

[22] Hamidreza Nemati and Allahyar Montazeri. Analysis and design of a multi-channel time-varying sliding mode controller and its application in unmanned aerial vehicles. *IFAC-PapersOnLine*, 51(22):244–249, 2018.

[23] Hamidreza Nemati and Allahyar Montazeri. Design and

development of a novel controller for robust attitude stabilisation of an unmanned air vehicle for nuclear environments. In *2018 UKACC 12th International Conference on Control (CONTROL)*, pages 373–378. IEEE, 2018.

[24] Panagiotis Radoglou-Grammatikis, Panagiotis Sarigiannidis, Thomas Lagkas, and Ioannis Moscholios. A compilation of uav applications for precision agriculture. *Computer Networks*, 172:107148, 2020.

[25] Abdul-Wahid A Saif and Imil H Imran. Control of yaw motion of nonlinear unmanned underwater vehicle over wireless network. In *2017 14th International Multi-Conference on Systems, Signals & Devices (SSD)*, pages 823–826. IEEE, 2017.

[26] Virginia Santamarina-Campos and Marival Segarra-Oña. *Drones and the Creative Industry: Innovative Strategies for European SMEs*. Springer Nature, 2018.

[27] Xingling Shao, Linwei Wang, Jie Li, and Jun Liu. High-order eso based output feedback dynamic surface control for quadrotors under position constraints and uncertainties. *Aerospace Science and Technology*, 89:
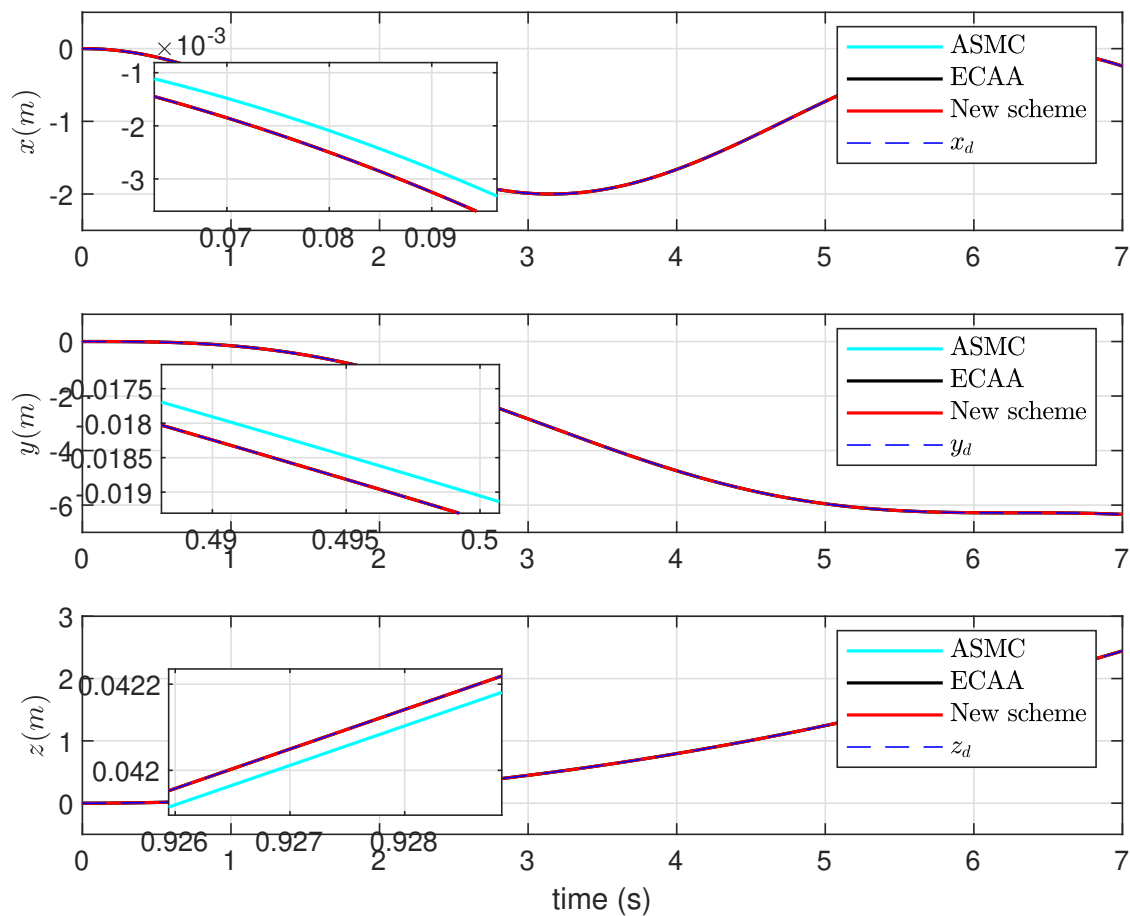
FIGURE 5: Profile of x, y and z.

288–298, 2019.

[28] Xingling Shao, Xiaohui Yue, and Jie Li. Event-triggered robust control for quadrotors with preassigned time performance constraints. *Applied Mathematics and Computation*, 392:125667, 2021.

[29] Jung-Sup Um. *Drones as Cyber-Physical Systems*. Springer, 2019.

[30] Holger Voos. Nonlinear control of a quadrotor micro-uav using feedback-linearization. In *2009 IEEE International Conference on Mechatronics*, pages 1–6. IEEE, 2009.

[31] Jing-Jing Xiong and Guobao Zhang. Discrete-time sliding mode control for a quadrotor uav. *Optik*, 127 (8):3718–3722, 2016.

[32] Qing-Li Zhou, Youmin Zhang, Camille-Alain Rabbath, and Didier Theilliol. Design of feedback linearization control and reconfigurable control allocation with application to a quadrotor uav. In *2010 Conference on Control and Fault-Tolerant Systems (SysTol)*, pages 371–376. IEEE, 2010.

[33] Zongyu Zuo. Trajectory tracking control design with command-filtered compensation for a quadrotor. *IET control theory & applications*, 4(11):2343–2355, 2010.

IMIL HAMDA IMRAN received the B.S. degree in Electrical Engineering from Andalas University, Indonesia, in 2011, the M.S. degree in Systems and Control Engineering from King Fahd University of Petroleum and Minerals, Saudi Arabia, in 2015, and the Ph.D. degree in Electrical Engineering from The University of Newcastle, Australia, in 2020. He was a Postdoctoral Research Associate at the Department of Engineering, Lancaster University, United Kingdom from April 2020 to February 2022. He is currently a Postdoctoral Fellow at the Applied Research Center for Metrology, Standards and Testing, King Fahd University of Petroleum and Minerals, Saudi Arabia. His research interests include networked control systems, multi-agent systems, nonlinear control and adaptive control.
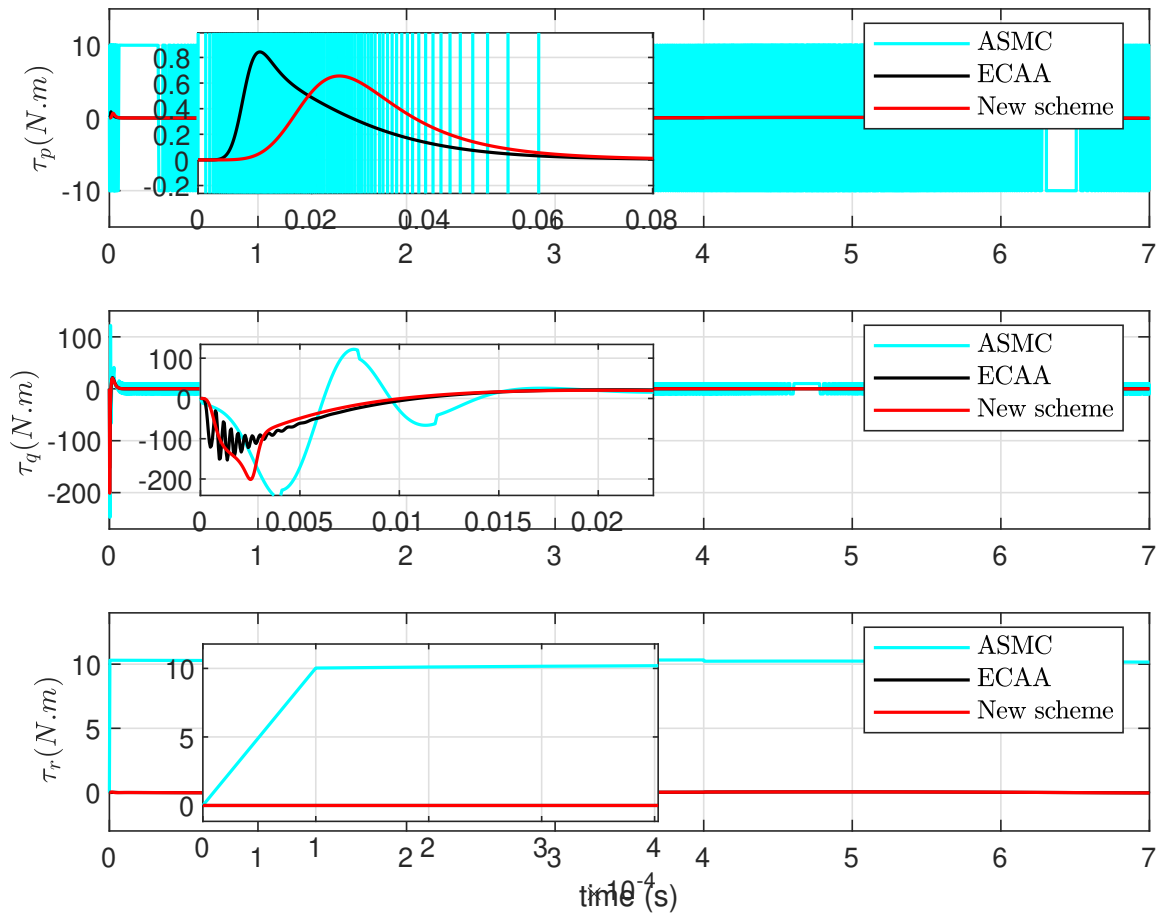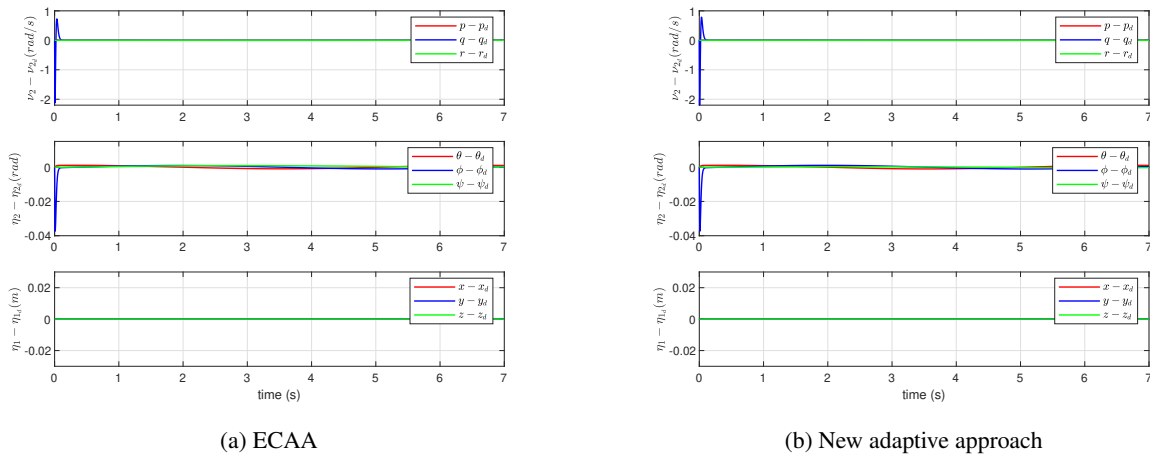
FIGURE 6: Profile of τ.

(a) ECAA

(b) New adaptive approach

FIGURE 7: Profile of the tracking trajectory errors.

(a) ECAA

(b) New adaptive approach
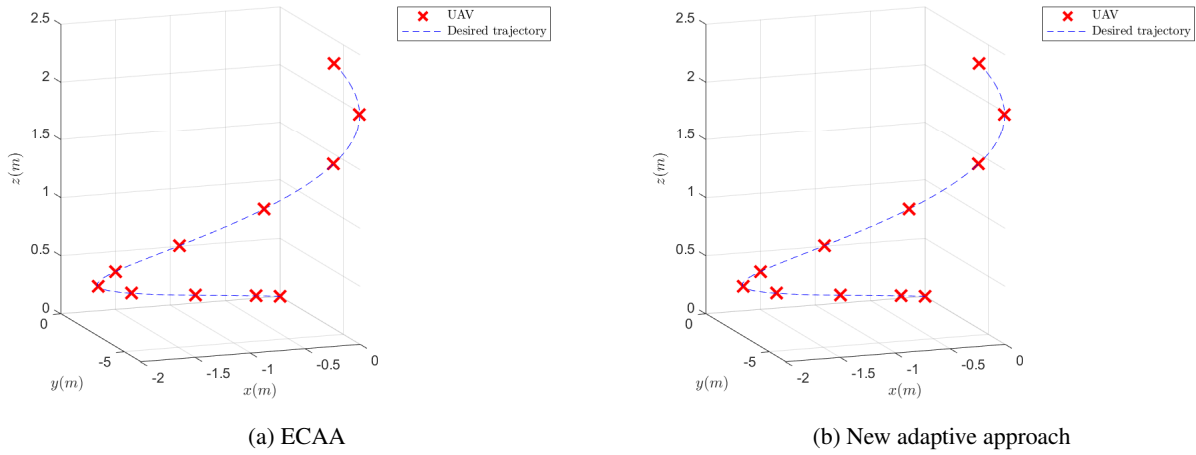
FIGURE 8: Profile of x, y and z in 3D.

(a) ECAA

(b) New adaptive approach
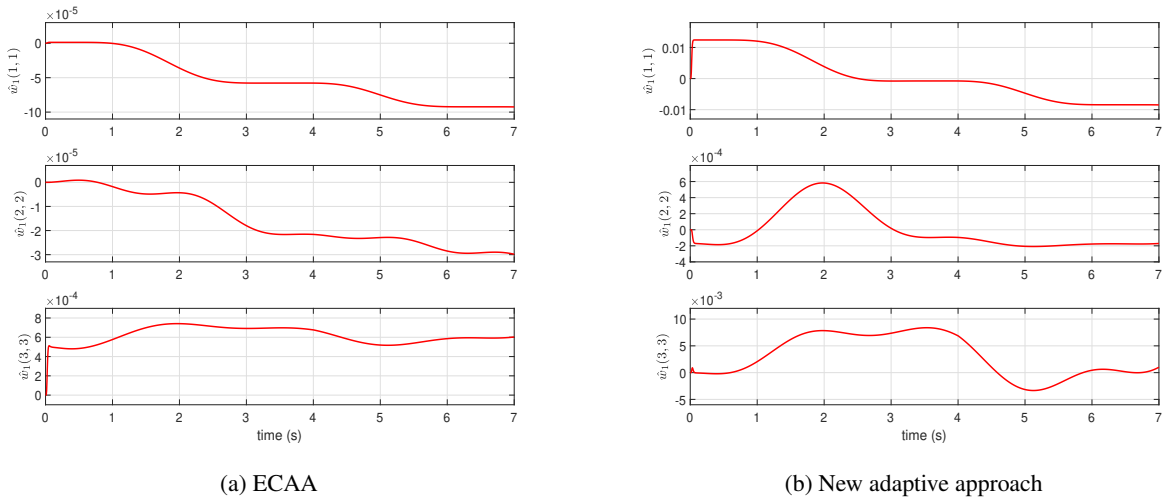
FIGURE 9: Profile of the state of adaptation law to handle w_1.

(a) ECAA

(b) New adaptive approach
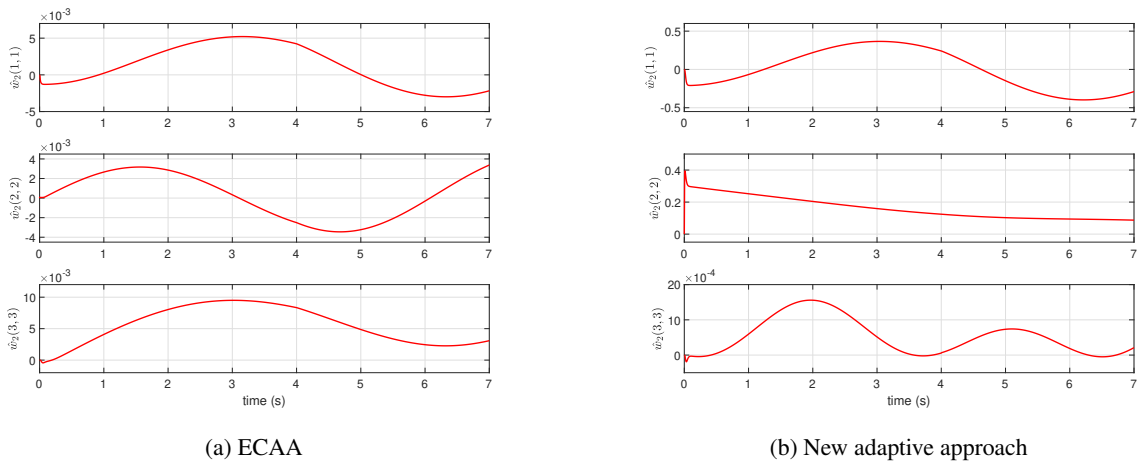
FIGURE 10: Profile of the state of adaptation law to handle w_2.

(a) ECAA

(b) New adaptive approach
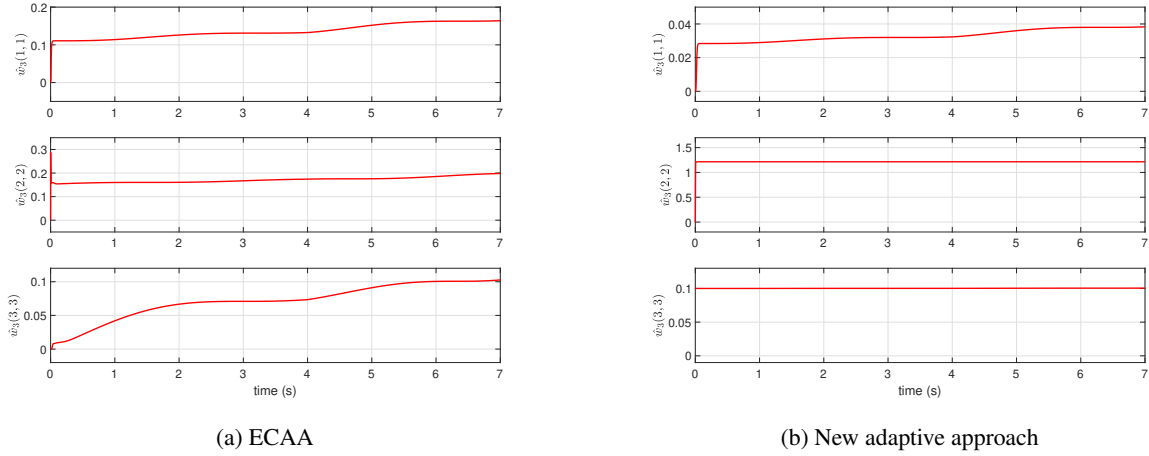
FIGURE 11: Profile of the state of adaptation law to handle w_3.

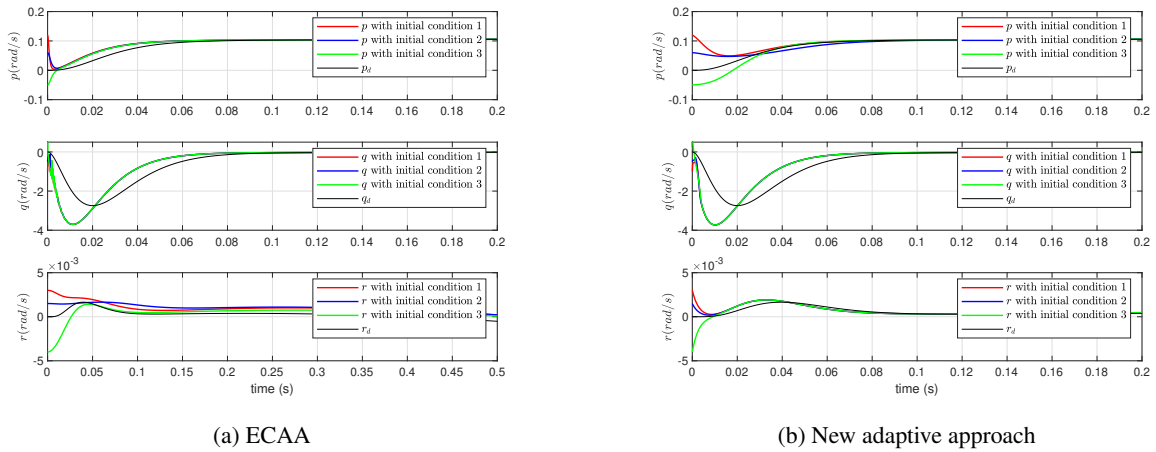(a) ECAA

(b) New adaptive approach

FIGURE 12: Profile of p, q and r with different initial conditions.

RUSTAM STOLKIN serves as the Chair in Robotics and Royal Society Industry Fellow in the School of Metallurgy and Materials. He leads the Extreme Robotics Lab (ERL), Europe's most prominent university research lab dedicated to nuclear and other extreme environment applications of advanced robotics and AI. Rustam is an interdisciplinary engineer with diverse research interests, although mainly focusses on robotics. His main interests include vision and sensing, robotic grasping and manipulation, robotic vehicles, human-robot interaction, AI and machine learning.

His training included undergraduate and masters degrees in Engineering from Oxford University, and a PhD in Robot Vision undertaken between University College London and UK imaging industry. He also worked as an Assistant Professor (Research) at Stevens Institute of Technology, USA, 2004-2008.

He is actively involved in applied robotics and imaging projects with industry. He currently has funded collaborations with nuclear industry, defence industry, industrial robotics industry, and manufacturing industry. He is also particularly interested in education and public communication of science, and has spent many years working with young people, in both UK and USA, teaching science through engaging hands-on activities with robotics. He has been teaching robotics master-classes for young people at Royal Institution of Great Britain over the past five years.

ALLAHYAR MONTAZERI was born in Tehran, Iran in 1978. He received the B.S. degree in electrical engineering from Tehran University, Tehran, Iran in 2000, and the M.Sc. and Ph.D. degrees in electrical engineering from Iran University of Science and Technology, Tehran, Iran, in 2002, and 2009, respectively.

Between 2010 and 2011, he joined the Fraunhofer Institute, Germany as a research fellow, and then carried on his research with Fraunhofer IDMT and control engineering group, Ilmenau University, Germany during the years 2011 to 2013. He has been the visiting research scholar with the control engineering group at ETH Zurich, Switzerland and the chemical engineering group in Norwegian University of Science and Technology (NTNU), Trondheim, Norway. Since 2013, he has been working as assistant professor with the Engineering Department at Lancaster University, United Kingdom. His research interests cover a wide range of areas on control theory and digital signal processing. Particularly he is interested in Adaptive Signal Processing and Control, Robust Control, Linear and Nonlinear System Identification, Estimation Theory, and Evolutionary Computing and Optimization with applications in Active Noise and Vibration Control Systems, Robotics.

Dr Montazeri is recipient of the European research consortium on informatics and mathematics (ERCIM) and Humboldt research awards in 2010 and 2011 respectively. He is also a fellow of higher education academy. His research is funded by different councils and industries in UK such as Engineering and Physical Research Council, Sellafield Ltd, National Nuclear Laboratory, and Nuclear Decommissioning Authority. He is currently serving as IFAC Technical Committees 'Adaptive and Learning Systems' and 'Modelling, Identification, and Signal Processing'.

. . .